C.P. No. 1341

PROCUREMENT EXECUTIVE, MINISTRY OF DEFENCE

AERONAUTICAL RESEARCH COUNCIL

CURRENT PAPERS

The Prediction of Helicopter Rotor Hover Performance using a Prescribed Wake Analysis

by

C. Young

Aerodynamics Dept., R.A.E., Farnborough

LONDON: HER MAJESTY'S STATIONERY OFFICE

1976

PRICE £2-00 NET

UDC 533.662.6 : 533.6.013.67 : 533.6.048.3 : 533.6.013.16 : 533.6.048.1

*CP No.1341
June, 1974

THE PREDICTION OF HELICOPTER ROTOR HOVER PERFORMANCE USING A PRESCRIBED WAKE ANALYSIS

by

C. Young

SUMMARY

A method of calculating the performance of a helicopter rotor in the hover is presented. The method combines the downwash velocity distribution induced by a contracting spiral vortex wake with strip element-momentum theory. The shape of the wake takes a prescribed geometry developed from an extensive series of model tests made in the USA.

The predicted thrust and power is in good agreement with measurements made on model and full scale rotors provided that the aerofoil data is sufficiently well defined. The calculated load distribution along the blade is also compared with measurements made on Wessex helicopters. The load distribution is shown to be very sensitive to a light wind but theory compares well with experiment when this effect is eliminated.

The hover performance predicted using only the wake induced velocity distribution is also discussed. The rotor performance is shown to be too sensitive to the geometry of the wake for the method to be used as a design tool with confidence, and the mathematical representation of the wake needs improving.

---

* Replaces RAE Technical Report 74078 - ARC 35652.

CONTENTS

1 INTRODUCTION

The modern turbine powered helicopter is more often limited by the thrust capability of the main or tail rotor than by a lack of available power. This limitation in forward flight is due to the blade stalling on the retreating side of the rotor disc, and is the reason for the growing trend towards aerofoil sections designed specifically for helicopter rotors[1] instead of the NACA 00 series aerofoils which have been used for so long. However, the potential benefits of using new blade profiles, or making other changes to the rotor geometry, can only be exploited effectively if the blade load distribution can be accurately calculated in all flight conditions.

The ideal blade geometry for high speed forward flight is unlikely to be ideal for efficient hover and the designer must reach a compromise solution. The final configuration will be achieved by giving different weightings to hover performance according to the tasks which the particular helicopter is expected to perform. A heavy lift, or crane helicopter, is likely to have its forward speed capability sacrificed for a more efficient hovering performance. An aerofoil section with a high usable lift coefficient at a Mach number of 0.6, a typical value for the blade tip in hover, would undoubtably be advantageous, but such an aerofoil is likely to have a low drag rise Mach number and shock induced separations would limit the Mach number of the advancing blade and hence the forward speed capability of the aircraft. In addition, the best twist distribution for hover is likely to be too large for high speed forward flight. However, the essence of the helicopter concept is its high efficiency as a hovering vehicle and a method of predicting the hover performance of a whole range of blade geometries and rotor configurations is essential.

The main problem in calculating the performance of a helicopter in hover is determining the induced flow velocity through the rotor. The simplest mathematical model of a rotor is the actuator disc in which the rotor is replaced by a disc having a pressure difference between the upper and lower surfaces. This concept can be used for forward flight or hover calculations but suffers from the disadvantage that the effect of changing the rotor parameters such as blade geometry, aerofoil section, solidity and tip speed cannot be investigated.

An improved model of the flow combines blade element and momentum theory. The radial variation of the induced velocity and hence the forces on the blade are better represented in this model making it suitable for initial design

studies, but the thrust to power relationship is not correctly predicted as the disc loading, tip Mach number, or solidity are increased. An excellent review of this method is given in Ref.2.

The simple methods fail because neither the wake from the blades nor the wake contraction are represented and these are particularly important in hover because the rotor is continually in the influence of its own wake. The most important feature of the wake is the strong tip vortex which contracts rapidly and passes just below the following blade. A large upwash is induced outboard of this vortex which opposes the mean downwash through the rotor to produce a high angle of attack in the tip region which can be sufficient to stall the blade at higher thrust levels.

Calculation methods using vortex wakes have appeared quite frequently in recent years and vary in sophistication from 'free wake' methods, in which the wake is allowed to distort under its own induced velocity field[3,4,5], to simpler methods where the wake takes a prescribed geometry[5]. The 'free wake' methods have the disadvantage of needing long computer runs making them unsuitable for parametric studies, and some of the results do not always compare favourably with experiment[5]. The prescribed wake approach uses much less computer time and can be made to give consistent results provided that the wake geometry has been determined accurately, and the mathematical representation of the wake is realistic. The method in this Report uses the wake geometry obtained by Landgrebe[5] from experiments on model rotors and is described in section 2.3. The downwash distribution induced solely by the vortex wake could not be used to determine the rotor performance for the reasons discussed in section 4, and it has to be linked to momentum theory. The method employed is similar to that used by Rorke and Wells[6] and is outlined in section 2.2.

The results of the theory are compared with measurements made on full scale rotors in free flight tests at RAE Bedford[9,10] and with results from model tests[5] and whirl stand tests[6] made in the USA. The comparisons presented in section 3 show that the theory gives accurate performance estimates for a wide range of configurations.

2 DESCRIPTION OF THE METHOD

2.1 The mathematical model of the flow

The basic method used in calculating the hover performance of a rotor is similar to that described elsewhere[3,6], and uses lifting line theory. The blades

are represented by bound vortex lines divided into a number of segments each having a different circulation strength corresponding to the variation of the radial load distribution. A trailing vortex filament must originate at the ends of the blade segments to satisfy the Helmholtz law of conservation of vorticity. These trailing vortex filaments, which represent the wake, take a prescribed contracting helical path below the rotor and are approximated in the theory by a series of short straight vortex elements. The strength of the trailing vortex filament is constant along its length and is equal to the difference in the circulation between two adjacent bound vortex segments, Fig.1.

The flow at the blade is assumed to be two-dimensional and the aerodynamic characteristics are evaluated at the midpoint of each blade segment using measured two-dimensional aerofoil lift and drag coefficients.

2.2 The wake-momentum analysis

The determination of the inflow angle or downwash velocity distribution is the major difficulty in predicting rotor hover performance. Landgrebe states[5] that the velocity induced solely by the wake may be used, but section 4 shows that this is unsatisfactory in practice. The wake induced velocity often overestimates the magnitude of the downwash distribution leading to high induced power factors, especially for rotors with a high disc loading. The predicted thrust to power relationship is improved if the wake induced velocity is factored by the ratio of the momentum value of downwash to the mean of the wake induced velocity, but this tends to overestimate the blade load distribution near the tip. A much closer integration of the wake induced velocity with momentum theory is required and is most easily obtained by using the wake-momentum analysis of Rorke and Wells[6]. Strip element-momentum theory is combined with the wake induced velocity to ensure that the thrust produced by each element of the blade is consistent with momentum theory.

The thrust, ΔT_i, produced by an element of the blade of length Δr_i centered on $\bar{r}_i$ is

$$\Delta T_i = \rho(2\pi \bar{r}_i \Delta r_i) v_i 2v_i \qquad (1)$$

from momentum theory, and

$$\Delta T_i = \tfrac{1}{2}\rho\left((\Omega \bar{r}_i)^2 + v_i^2\right) b c_i \Delta r_i \left[C_{L_i} \cos \eta_i - C_{D_i} \sin \eta_i\right] \qquad (2)$$

from strip element theory, where $\eta_i = \tan^{-1}(\nu_i/\Omega\bar{r}_i)$ is the inflow angle, and ν_i is the downwash velocity. This velocity is positive contrary to the usual definition which is employed later. The value of η_i can be found at all radial stations by equating equations (1) and (2) and solving by iteration. An iterative solution is necessary because C_{L_i} and C_{D_i}, the two-dimensional aerofoil lift and drag coefficients evaluated at the appropriate Mach number, depend on η_i since the local angle of incidence of the blade α_i is

$$\alpha_i = \theta_R + \theta_i - \eta_i$$

where θ_R is the collective pitch and θ_i is the blade twist. The solution of equations (1) and (2) represents the usual strip element-momentum theory without a tip loss factor, and this downwash distribution is used as the starting point in the present calculation. For this reason it will be referred to as the initial momentum downwash distribution.

The wake induced velocity distribution v_i is introduced as an interference velocity Y_i defined in the present method as the difference between the wake induced velocity and the initial momentum downwash velocity,

$$Y_i = -v_i - \nu_i \quad .$$

The negative sign appears on the wake induced velocity because it is calculated in the conventional sense of downwash negative, whereas Y_i is defined in the same sense as ν_i. Defining

$$\beta_i = \tan^{-1}\frac{Y_i}{\Omega\bar{r}_i}$$

the thrust given by momentum theory is modified to

$$\Delta T_i = \rho(2\pi\bar{r}_i\Delta r_i)(Y_i + w_i)2w_i \qquad (3)$$

and for strip element theory

$$\Delta T_i = \tfrac{1}{2}\rho\left((\Omega\bar{r}_i)^2 + (Y_i + w_i)^2\right)bc_i\Delta r_i\left[C_{L_i}\cos(\beta_i + \phi_i) - C_{D_i}\sin(\beta_i + \phi_i)\right] \qquad (4)$$

where $\phi_i = \tan^{-1}(w_i/\Omega\bar{r}_i)$.

The new value of the momentum downwash velocity w_i is found by solving equations (3) and (4), and is not to be confused with the initial momentum downwash used in the definition of the interference velocity.

There will be exact agreement between the thrust from momentum theory and strip element theory when equations (3) and (4) are equal, i.e. when

$$\frac{8\pi\bar{r}_i}{bc_i} \frac{(\beta_i + \phi_i)\phi_i}{\left[C_{L_i} \cos(\beta_i + \phi_i) - C_{D_i} \sin(\beta_i + \phi_i)\right]} - 1 = 0 \quad . \qquad (5)$$

The value of ϕ_i can be found from this equation by an iterative solution since the aerofoil lift and drag coefficients now depend on both β_i and ϕ_i. The local blade angle of incidence is

$$\alpha_i = \theta_R + \theta_i - (\beta_i + \phi_i)$$

but the collective pitch is not the same as in the initial calculation without the interference velocities since it is adjusted so that the total rotor thrust is the same in both cases.

The total downwash velocity distribution along the blade u_i, now becomes, in the conventional sense

$$u_i = -\Omega\bar{r}_i(\tan\beta_i + \tan\phi_i) \quad .$$

2.3 The wake geometry

The most comprehensive investigation of the wake geometry from a hovering rotor is that reported by Landgrebe in Ref.5. Tests were made on model rotors with up to eight blades with varying twist, aspect ratio and rotational speed, over a range of thrust levels up to blade stall. Overall thrust and power was measured, and the wake made visible by injecting smoke from a rake. A set of parameters relating the wake geometry to the rotor thrust coefficient, solidity, and blade twist was obtained from photographs taken of the wake against a reference grid. These parameters or coefficients allow a wake to be quickly established for any given rotor conditions. Comparisons of the wake generated by this method show good agreement with measurements made on wakes from full scale rotors and those predicted by some 'free wake' calculations.

The model rotor used in the experiments had a radius of 0.679 m. All the blades had a NACA 0012 aerofoil section, a chord length of 37.3 mm or 49.8 mm, and a rectangular tip. The flapping hinge offset was 6.8% R and the root cut out of the blades was 14.8% R.

The main rotor parameters investigated in the experimental programme were:

Number of blades	2, 4, 6, 8
Linear twist	0, -8°, -16°
Solidity ratio	0.035 to 0.1867
Tip speed	160, 183, 213 m/s
Tip Mach number	0.46, 0.525, 0.61
Blade aspect ratio	18.2, 13.6 .

Combinations of all these parameters were not tested but sufficient configurations were used to produce a consistent set of generalised wake coefficients.

The wake from a hovering rotor can be divided into two distinct parts, an inboard vortex sheet, and a strong, rolled up tip vortex. The vortex sheet, which is approximated in the theory by a number of vortex filaments, moves down rapidly below the rotor disc, the vertical displacement varying linearly with radius. The tip vortex rolls up very rapidly and remains close to the tip path of the blades until the following blade approaches when it moves down more rapidly though still not as quickly as the outer part of the vortex sheet, Fig.2. Landgrebe therefore gives different wake coefficients for the two parts of the wake.

The tip vortex vertical displacement, $\bar{z}$ is given by

$$\bar{z} = \begin{cases} K_1\psi & 0 \leqslant \psi \leqslant \psi_b \\ K_1\psi_b + K_2(\psi - \psi_b) & \psi > \psi_b \end{cases}$$

where ψ is the azimuth position measured from the blade, and ψ_b is the azimuth separation of the blades. The wake geometry coefficients K_1 and K_2 are

$$K_1 = -0.25(C_T/s + 0.001\theta_1)$$

$$K_2 = -(1.41 + 0.0141\theta_1)\sqrt{C_T/2}$$

where θ_1 is the blade twist in degrees. The tip vortex radial coordinate $\bar{r}$ is

$$\bar{r} = 0.78 + 0.22e^{-\lambda\psi}$$

with

$$\lambda = 0.145 + 27\ C_T \quad .$$

The vortex sheet vertical displacement varies linearly with radius and can be imagined as part of a line extending from the axis of rotation $\bar{r} = 0$, to a cylinder whose radius is equal to the rotor radius, $\bar{r} = 1$. The vertical displacement at the ends of the imaginary line is

$$\bar{z}_{\bar{r}=0} = \begin{cases} 0 & 0 \leq \psi \leq \pi/2 \\ K_{20}(\psi - \pi/2) & \psi > \pi/2 \end{cases}$$

$$\bar{z}_{\bar{r}=1} = \begin{cases} K_{11}\psi & 0 \leq \psi \leq \psi_b \\ K_{11}\psi_b + K_{21}(\psi - \psi_b) & \psi > \psi_b \end{cases}$$

where $K_{20} = \theta_1/128\ (0.45\theta_1 + 18)\sqrt{C_T/2}$

$K_{11} = -\ 2.2\ \sqrt{C_T/2}$

$K_{21} = -\ 2.7\ \sqrt{C_T/2}$.

The radial displacement $\bar{r}$ of a point on the vortex sheet originating from a point r_A say, on the blade is found by evaluating the vertical displacement of the sheet using the expressions above, then

$$\bar{r} = \frac{r_A r_T}{R}$$

where r_T is the radial location of the tip vortex at the point at which it has the same vertical displacement as the point on the vortex sheet.

The generalised wake coefficients generate a wake on the form shown in cross section in Fig.2. This figure shows one revolution of the wake for a six bladed rotor at a moderate thrust coefficient.

The roll up of the tip vortex is simulated by allowing all the trailing vortex filaments that originate outboard of the blade segment with the largest value of circulation strength to merge after one azimuth interval, typically 30^{o}. This is clearly shown in Fig.1 where four vortex filaments merge to form the tip vortex.

The rotor performance predicted using the generalised wake geometry was shown in Ref.5 to be very sensitive to small changes in the position of the tip vortex. This sensitivity is not so apparent in the present method because the induced downwash velocity is locally matched to the momentum velocity.

The wake produced by the wake coefficients neglects tip vortex instability, vortex dissipation and asymmetry of the wake, all of which are likely to be present when the rotor is operating in its real environment. Some recent experiments[7] have shown that adjacent tip vortices interact and eventually dissipate by mutual interference, and others[6,7] using theoretical methods have found that the far wake can be unstable. These phenomena generally occur some distance below the plane of the disc and do not invalidate the argument that the most important effect of the wake on rotor performance is the close passage of the tip vortex from the preceding blade. Wake asymmetry occurs because the loading on all the blades is not the same. This is almost bound to happen in practice because of small differences in the manufactured blades, atmospheric turbulence, and light winds, all of which will distort the wake and degrade the performance of the rotor by increasing the blade load near the tips[10]. The rotor performance predicted using the generalised wake can therefore be regarded as ideal since it cannot represent real conditions but such calculations are still of great importance to the helicopter designer.

The range of the model tests was quite extensive but all the blades had a constant chord, linear twist and rectangular tips, and the range of blade aspect ratio was quite small. The wake geometry does not appear to be sensitive to aspect ratio and most of the full scale rotors for which comparisons are made in section 3 have aspect ratios which lie outside the range of the model tests. Accurate performance estimates for tail rotors have also been obtained using the generalised wake geometry although these rotors have higher solidity ratios than the models and are operated at greater thrust coefficients. It seems likely that the generalised wake is applicable to a wider range of parameters than those

tested, but excursions outside the range of the test programme have been approached with caution. The use of the wake geometry for tapered blades, blades with non-linear twist distributions or peculiar tip shapes has not been attempted, and the present wake model is unlikely to be suitable for these configurations.

2.4 The performance calculation

The sequence of operations in the performance calculation as implemented on a digital computer is shown in the form of a flow diagram in Fig.3. It is an iterative process which is converged when the radial load distribution changes by less than a certain tolerance between two successive iterations. Convergence of the load distribution implies that the bound and trailing vortex strengths, and the interference velocities have also converged.

The data required consists of the geometry of the rotor, i.e. the twist, chord and mass distributions, the rotor rotational speed, the air density, the local speed of sound, and the required rotor thrust. The two-dimensional aerofoil data is supplied in the form of tables listing the measured lift and drag coefficients at angles of attack up to the stall for a range of Mach numbers. Other input variables define how the wake is to be set up in terms of the number of wake revolutions, and the number of short vortex line elements representing each revolution of the wake.

The blade is specified at $n + 1$ radial positions, r_i, with r_1 at the root cut out, and r_{n+1} at the tip. These points define the ends of the bound vortex segments and are spaced more closely in the tip region of the blade where the loading changes most rapidly. The midpoints of the segments, $\bar{r}_i$, are then associated with a value of the blade chord c_i, and twist θ_i, obtained from the input data by linear interpolation.

The first iteration loop starts by evaluating the initial momentum value of the downwash distribution using equations (1) and (2). On subsequent iterations, the interference velocities will be known and equation (5) is used to calculate the downwash distribution. The appropriate lift and drag coefficients at the midpoints of the blade elements are evaluated using either equations (1) and (2), or equation (5) so the thrust and torque distributions T_i, Q_i can be calculated immediately,

$$T_i = \tfrac{1}{2}\rho\left[C_{L_i}\Omega\bar{r}_i + C_{D_i}u_i\right]V_i c_i$$

$$Q_i = \tfrac{1}{2}\rho\left[C_{D_i}\Omega\bar{r}_i - C_{L_i}u_i\right]V_i c_i\bar{r}_i$$

where $V_i = \sqrt{(\Omega\bar{r}_i)^2 + u_i^2}$, and u_i is the downwash velocity evaluated in the conventional sense.

The thrust and torque distributions are integrated and multiplied by the number of blades to give the total rotor thrust and torque. The calculated thrust is compared with the required value and, if necessary a correction is made to the collective pitch. The calculation is then repeated until the calculated and required thrust agree to within a specified tolerance.

The coordinates of the blades and wake are set up in a Cartesian coordinate system to facilitate the calculation of the wake induced velocity components. The blade coning angle a_0 is,

$$a_0 = \sin^{-1}\left\{\frac{g(M_A - M_b)}{\Omega^2(I_b + eM_b)}\right\}$$

where M_A is the aerodynamic moment about the flapping hinge, M_b and I_b are the first and second moments of inertia of the blade about the flapping hinge, and e is the hinge offset length. The coordinates of the points defining the blades then become

$$x_{ki} = (e + (r_i - e)\cos a_0)\cos\psi_k$$

$$y_{ki} = (e + (r_i - e)\cos a_0)\sin\psi_k$$

$$z_{ki} = (r_i - e)\sin a_0$$

where $\psi_k = (k - 1)\,2\pi/b$, $k = 1, \ldots b$, and r_i is the radial position on the reference blade at $\psi = 0$, $y = 0$.

The near wake is set up using the generalised wake geometry described in section 2.3. The number of vortex filaments that merge to form the tip vortex will not be known for the first iteration, but this number can be specified in the input data if it is known from a similar calculation, or can be crudely

calculated in the computer program. Normally the spiral wake is only allowed to develop for about four revolutions when it is nearly fully contracted, and the far wake for each vortex filament is represented by ten inclined vortex rings separated vertically by a distance equivalent to one revolution of the wake.

There are two main methods of using the radial load distribution to calculate the strength of the bound vortex distribution. The simple method is to set

$$\Gamma_i = \tfrac{1}{2}\Omega \bar{r}_i C_{L_i} c_i$$

but this has the disadvantage that the maximum value of circulation strength, and thus the peak value of the blade load, always occurs on the last blade segment, typically at 98% radius, which is not observed experimentally. The method used in the present calculation is similar to that of Piziali and Du Waldt[8] and has the advantage of calculating the shape of the vortex distribution, though not its final converged level, almost immediately because the equations contain terms that depend on the wake geometry. Thus the blade element with the maximum circulation strength calculated even with the initial radial load distribution is in approximately the correct position. In this respect, the calculation anticipates the induced velocity distribution which is used for the next iteration. The basic method of Ref.8 has to be modified, however, because the downwash velocity distribution has two contributions, the wake interference velocity Y_i, and the momentum velocity w_i, instead of just the wake induced velocity in the original method.

The general relation between the strength of the bound vortex Γ_i and the lift on the blade segment is

$$\rho \Omega \bar{r}_i \Gamma_i = \tfrac{1}{2}\rho (\Omega \bar{r}_i)^2 C_L c_i$$

i.e.

$$\Gamma_i = \tfrac{1}{2}\Omega \bar{r}_i C_L c_i \quad .$$

The lift coefficient C_L is expanded in a form which makes it possible to separate the terms depending on the wake geometry so they may be combined on the left hand side of the equation with the vortex strength. The lift coefficient in the above expression is replaced at each radial station by

$$C_L = C_{L_i} + \left(\frac{\partial C_L}{\partial \alpha}\right)_i \left[\theta_R + \theta_i - \alpha_i + \frac{u_i}{\Omega \bar{r}_i}\right]$$

where C_{L_i} is the calculated lift coefficient and the term in square brackets (which is nominally zero if the previous calculated value for u_i is taken) is to be split up. The lift curve slope of the aerofoil $(\partial C_L/\partial \alpha)_i$ is evaluated near α_i at the Mach number appropriate to the ith point on the blade. The downwash velocity u_i is

$$u_i = -\Omega \bar{r}_i (\tan \beta_i + \tan \phi_i)$$

and

$$\beta_i = \tan^{-1}\left(\frac{-v_i}{\Omega \bar{r}_i}\right) - \eta_i$$

thus

$$u_i = v_i + \Omega \bar{r}_i (\tan \eta_i - \tan \phi_i)$$

and substituting gives

$$\Gamma_i - \tfrac{1}{2} c_i \left(\frac{\partial C_L}{\partial \alpha}\right)_i v_i = \tfrac{1}{2} \Omega \bar{r}_i c_i \left\{C_{L_i} + \left(\frac{\partial C_L}{\partial \alpha}\right)_i \left[\theta_R + \theta_i - \alpha_i + \tan \eta_i - \tan \phi_i\right]\right\} .$$

The important step now is to express the wake induced velocity v_i, in terms of a function depending only on the wake geometry and the values of the bound vortex strength (which have yet to be evaluated) since the strength of the trailing vortex filaments γ_j is equal to the difference in the value of the adjacent bound vortex segments. Thus,

$$v_i = \sum_{j=1}^{n+1} \sigma_{ij} \gamma_j$$

but

$$\gamma_j = \Gamma_{j-1} - \Gamma_j$$

therefore

$$v_i = \sum_{j=1}^{n} (\sigma_{ij+1} - \sigma_{ij}) \Gamma_j$$

where σ_{ij} is an influence coefficient which depends only on the wake geometry and when multiplied by the trailing vortex strength is the total velocity induced at the midpoint of the ith blade segment by the jth vortex filament from all the blades. A system of simultaneous linear equations can be written down

$$\Gamma_i - \tfrac{1}{2}c_i\left(\frac{\partial C_L}{\partial \alpha}\right)_i \sum_{j=1}^{n} (\sigma_{ij+1} - \sigma_{ij})\Gamma_j =$$

$$\tfrac{1}{2}\Omega \bar{r}_i c_i \left\{ C_{L_i} + \left(\frac{\partial C_L}{\partial \alpha}\right)_i \left[\theta_R + \theta_i - \alpha_i + \tan \eta_i - \tan \phi_i\right]\right\} \qquad i = 1, \ldots n$$

which can be solved for the unknown vortex strengths Γ_i . The present method uses matrix inversion and multiplication to solve the equations.

A very rapid calculation follows from using this method of solving for the circulation strengths combined with the collective pitch iteration to ensure that the rotor thrust is nominally the same for each iteration. The wake geometry, for a particular rotor configuration depends only on the rotor thrust coefficient and will not therefore change significantly between iterations. The only feature of the wake that may change is the number of vortex filaments that roll up to form the tip vortex. The method of calculating the vortex strengths gives the shape of the distribution and in particular, the radial position of the blade segment with the highest value of circulation strength during the first few iterations. The wake geometry therefore remains virtually unchanged throughout the calculation and the more time consuming computations can be omitted. When the wake geometry has converged, there is no need to set up a new wake on each iteration, and new influence coefficients are not calculated as these depend solely on the wake geometry. A new circulation matrix has to be formed and inverted during each iteration but this uses the set of influence coefficients calculated when the final wake was set up together with the latest calculated values of the aerofoil lift curve slope. There will also be a new set of variables on the right hand side of the equations but the time required for these matrix operations is small compared to that required for calculating the wake geometry and influence coefficients. The other saving in time occurs because the wake induced velocities can be simply calculated from the existing influence coefficients and the latest calculated values of the trailing vortex

strengths. Normally only two or three iterations are needed for wake convergence and subsequent iterations can be made very rapidly. A check however is always made during every iteration to ensure that the blade element with the largest circulation strength has not changed which would then require a new wake geometry.

The interference velocity distribution is calculated from the wake induced velocities and the whole process repeated until the load distribution converges. The rotor performance is then printed out.

A typical calculation for a six bladed rotor with two main iterations to give wake convergence and a further twenty five iterations for a converged load distribution require about 35 seconds on a CDC 6600 computer.

3 COMPARISON BETWEEN THEORY AND EXPERIMENT

The rotor thrust and torque predicted by the theory have been checked against experimental results obtained from model tests[5], whirl stand tests[6], tethered helicopter tests and free flight helicopter tests[9]. The calculated load distribution has also been compared with some measurements made on Wessex helicopters in free flight[10,11].

All types of experimental techniques for investigating rotor hover performance require steady atmospheric conditions with little or no wind. Wind speeds of up to 4 m/s do not appear to have a large influence on the power required to produce a given thrust, but the blade load distribution can be significantly changed by even a very light wind. Model tests suffer least from unsteady conditions as the rotor environment can be carefully monitored and there is normally no difficulty in repeating suspect data points. The test room, however, must be large enough to avoid recirculation effects, and the low Reynolds number of the flow may not always be ideal for aerodynamic purposes. Results from whirl stands have to be corrected for ground effect and whirl stand interference; calm atmospheric conditions are essential. The problems associated with light winds can be partially avoided in free flight tests by flying the aircraft near a puff of smoke or observing the motion of a ball suspended on a light string below the helicopter. The tethered hover technique can also give accurate results since a range of rotor thrust levels can be covered quickly. Individual data points can be measured in carefully controlled tests with an accuracy of about 2% using good quality instrumentation, but a series of data points generally show a large scatter.

The source of the two-dimensional aerofoil data required by the performance calculation is important especially when the advantages of changing to a new aerofoil section for the blades is being investigated. The experimental data for the different aerofoils should ideally be obtained from tests in the same wind tunnel with the same amount of transition fixing on the aerofoil. The aerofoil data sometimes needs to be corrected as there can be some difference in the aerodynamic performance of the smooth aerofoil surface tested and the actual rotor blade which may be fitted with anti-erosion and de-icing strips or trailing edge tabs[15].

The usual method of testing a two-dimensional aerofoil in the UK is in a transonic wind tunnel with slotted or perforated walls, and with transition fixed to ensure that the boundary layer on the aerofoil is turbulent before the shock wave. The aerofoil drag coefficient is normally measured by a wake traverse. Results from wind tunnel tests made in the USA have often shown unrealistically low drag coefficients at low angles of attack because transition has not been fixed. Other results obtained by strain gauging a floating section of the aerofoil can also be unreliable because of poor sealing around the slots of the measuring station. The source of the aerofoil data used in the calculations is quoted for each example, and the details of the rotor geometry are also given as these have not always been easy to obtain.

3.1 Two bladed model rotor

The experimental data for the two bladed model rotor was obtained by Landgrebe[5] during the tests to derive the generalised wake geometry. The rotor chosen had blades with an eight degree linear twist and a chord length of 49.8 mm giving a solidity ratio of 0.0466, and a blade aspect ratio of 13.6. The tip speed was 213 m/s corresponding to a rotor rotational speed of 3000 rpm. The other geometric details of the rotor are given in section 2.3.

The two-dimensional aerofoil data for the NACA 0012 aerofoil used in the calculations has also been taken from Ref.5 (Fig.90), and are based on measured low Reynolds number data which has been synthesised to provide a correlation between the test results for the untwisted, two bladed model rotor and the results predicted by blade element-momentum theory. The resulting data has a high value of lift curve slope and are rather sparse. The variation of lift coefficient with angle of attack is shown for only three Mach numbers and the data required in the tip region, where the Mach number is about 0.6, falls

between two of the published curves making interpolation unreliable. These were, however, the only data available at the Reynolds number appropriate to the model tests, and any error introduced by reading from the small scale figures should not be too important for a rotor with only two blades.

The predicted thrust and torque is compared with the experiments in Fig.4. Agreement is good over the whole range of thrust levels and differs little from the results predicted by strip element-momentum theory. This is not surprising as the tip vortex from the preceeding blades lies well below the path of the following blade, and the angle of attack distribution shows very little distortion in the tip region. The correlation of thrust with collective pitch is not very good for this example and is about the same as that shown in Ref.5. This is probably a consequence of the higher lift curve slope of the synthesised aerofoil data rather than errors in the original data on which they were based[5].

3.2 Wessex main and tail rotors

The experimental results presented in this section have all been made on a Wessex helicopter. The predicted thrust and power for the main rotor is compared with measurements made in free flight at RAE Bedford[9]. The load distribution on the blade in the tip region was measured using another modified Wessex also at RAE Bedford[10], and along the complete blade in tests made in the USA[11]. The data for the tail rotor was obtained from wind tunnel tests[12] and free flight tests[9].

The four bladed main rotor of the Wessex has a radius of 8.53 m. Each blade has a linear twist of eight degrees, a NACA 0012 aerofoil section and a chord length of 0.417 m, giving a solidity ratio of 0.06216. The root cut out is 16% radius, and the flap hinge offset is 0.3 m. The tail rotor has a radius of 1.448 m with four untwisted blades of chord length 0.1865 m and again, a NACA 0012 aerofoil section. The flap hinge offset is 0.067 m and the root cut out of the blades has been assumed to be 31% radius. The tip speed of both rotors varies slightly throughout the flight envelope and a value of 205 m/s has been used when the actual value is not known.

The two-dimensional aerofoil data for the NACA 0012 aerofoil was measured in the NPL 36in × 14in transonic tunnel on a model with a chord length of 0.254 m [13]. Transition was fixed on the upper and lower surfaces by a band of carborundum extending from the leading edge to 2% chord. The lift coefficient was calculated by integrating the pressure distribution measured at 43 chordwise stations and the drag coefficient obtained by a wake traverse.

The thrust and torque coefficients for the main rotor measured in flight by Brotherhood[9] are compared with the theory in Fig.5. The experimental results were obtained on three different days with the rotor thrust coefficient varied mainly by changing the altitude of the aircraft. The theoretical results were also calculated by altering the density altitude and are shown with and without a vertical drag correction. If vertical drag is assumed to be 4% of the rotor thrust at low thrust increasing in proportion to the square of the mean value of downwash velocity at higher thrust levels, then excellent agreement between theory and experiment is obtained.

Another Wessex helicopter at RAE Bedford was used to compare the performance in flight[10] of the new RAE (NPL) 9615 aerofoil section designed for the Lynx helicopter, with the standard NACA 0012 profile. Two opposite blades were fitted with balsa wood and fibre glass fairings or gloves over the outer 12% of the blade, one glove shaped to the NACA 0012 section, the other to the new profile. The chord length of the gloves was increased to 0.47 m to retain the correct thickness/chord ratio of the aerofoils. Pressure tubes connected to tappings in the gloves were led along the blade to a scanivalve mounted on top of the rotor hub. The drag of the aerofoils was also measured at two radial stations by rakes fitted behind the trailing edge of the blades. The time averaged pressures measured at four radial positions on each of the blades were integrated to give the aerofoil lift coefficient and the blade load.

The load distribution on a helicopter blade is very difficult to measure in true hovering flight. A small amount of cyclic pitch will always be present to keep the aircraft in trim, and a slight wind will distort the path of the tip vortices and give asymmetric loading which itself changes the structure of the wake[7]. In the RAE tests, a few pressure transducers were also mounted in one of the gloves to give instantaneous pressures near the leading and trailing edge of the blade, and these show large variations, with azimuth, in local incidence near the tip. In some cases the loading was almost doubled and the aerofoil was operating for some of the time beyond the steady state stall boundary. Riley[10] has developed a simple analysis to estimate the change in the blade angle of incidence that occurs when the tip vortex is displaced from its expected position by a light wind. The analysis predicts the change in the angle of incidence quite well, and one example, using a wind speed of only 2.5 m/s showed a positive increase in incidence for over 280° of the disc with an increase of over 2° near the 90° azimuth position. Thus the blade load

distribution measured near the tip using a time averaged technique is expected to be higher than predicted. This is the case with the comparison shown in Fig.6. The theoretical curve is the correct shape near the tip but the loads are too low. The difference between the measured and calculated load, however, is the correct order of magnitude if it can be solely attributed to a light wind. A change in the angle of incidence of about 1.5^{o} would be sufficient to raise the predicted load at 95% radius to the measured value, and this is similar to the mean of the incidence change from Riley's analysis. The comparison is further complicated by the geometry of the blades used on the helicopter. Two of the blades had an increased chord which cannot be represented in the theory, but a calculation with all four blades having the same geometry as the two helicopter blades with the increased chord, has been made and the results are also shown in Fig.6. The theory now predicts a higher load but it is still less than that measured in flight.

A better comparison between theory and experiment can be made using the results from some flight tests made in the USA on a S-58 helicopter[11] which has an identical rotor system to the Wessex. The helicopter was again hovering in a light wind and the blade load at 95% radius varies by over 50% from 3.75 N/mm to 5.85 N/mm, but instantaneous pressures were recorded and the azimuthal variation of the blade load is known. Riley's analysis shows that the increment in the angle of incidence near the tip is zero at azimuth positions of about 40^{o} and 320^{o} when the wind is blowing from an azimuth angle of 180^{o} with a speed of 2.5 m/s. The actual wind speed is not specified in Ref.11 but it is probably of this order, and Cook[14] has shown that the wind is coming from an azimuth angle of 210^{o}. The increment in incidence due to the wake distortion would therefore be zero at 140^{o} on either side of this angle, i.e. at 70^{o} and 350^{o}. An examination of the blade cyclic and collective pitch angles show that the measured blade pitch is equal to the calculated collective pitch at azimuth angles of 58.9^{o} and 356.3^{o}, quite close to the positions where the increment in incidence is zero according to Riley. The calculated load distribution has therefore been compared with the mean of the load measured when the measured and calculated pitch angles are the same. This comparison, Fig.7, shows much better agreement especially in the tip region of the blade.

The above interpretation of the measurements is only one of the several possibilities. Hovering in a light wind, which is probably the situation most commonly encountered in 'hovering' flight, is a difficult situation to analyse

satisfactorily. It is unlikely that a wake cross section that is truly representative of the hover condition will coincide with the azimuth position where the effect of the wake distortion is zero. However, it is encouraging that the theory always predicts a blade load that is close to the mean of the measurements even though the load distribution may be varying by up to 100% near the tip.

The performance of the Wessex tail rotor has been compared with measurements made in the 24ft wind tunnel at RAE Farnborough[12] and with free flight tests made at RAE Bedford[9]. The wind tunnel tests were made on a complete aircraft fin assembly and the thrust measured was the resultant force on the fin, i.e. pure tail rotor thrust degraded by fin blockage and interference. A check on the performance of the tail rotor in isolation is not therefore possible. A comparison of the results, however, does give a measure of the fin blockage effect. Fig.8 shows that the additional power required to produce the extra thrust to overcome the blockage varies from 10% at low thrust levels to over 20% at higher thrusts. The power increment is expected to increase in this manner because the tail rotor mounted on the fin is working more into the drag rise and stall region of the aerofoil than the tail rotor in isolation.

The free flight tests show, Fig.8, an even greater power required to produce a given resultant thrust, or alternatively, a larger loss of thrust at the same torque as measured in the tunnel experiments. This can be due to several effects such as the main rotor wake impinging on the tail boom, or a light wind increasing the force on the fin or interference between the main rotor wake and the tail rotor flow, though it would be difficult to separate these effects. It seems unlikely that the tail rotor itself is behaving very differently especially as the measured collective pitch agrees so well with theory, Fig.9. These results suggest that tail rotors should be designed to have a large reserve of thrust to compensate for interference effects.

3.3 Sea King main and tail rotors

Tethered hover tests have been made on a Sea King helicopter by Westland Helicopters Ltd., and are used in this section for comparison with theory.

The main rotor blades of the Sea King have a NACA 0012 aerofoil section, a chord length of 0.463 m, a linear twist of eight degrees and a radius of 9.449 m. The tail rotor has a radius of 1.574 m with untwisted blades of chord length 0.186 m and a NACA 0012 aerofoil section. The flap hinge offset and

and root cut out of the main rotor are 0.321 m and 1.039 m and the corresponding figures for the tail rotor are 0.101 m and 0.488 m. The normal tip speed of the rotors, both of which have five blades, is 207 m/s.

The separate contributions to the total aircraft power were not measured and the following procedure, recommended by the manufacturers, has been adopted in calculating the total power demand. The torque required by the main rotor for a specified thrust was calculated using the aerofoil data of Ref.13, Fig.10. The tail rotor thrust required to counteract the main rotor torque was increased by 9% to allow for fin blockage, and the tail rotor torque calculated, Fig.11. The values of torque were converted to power and the total increased by 4% to allow for transmission losses. The power required by the electrical and hydraulic systems was represented by an additional 56 kW, independent of the rotor thrust, and, finally, the rotor thrust was reduced by 4% for vertical drag to give the aircraft weight. The total power and aircraft weight were then reduced to coefficient form using the main rotor radius and rotational speed. The comparison of the measured and calculated hover performance of the aircraft is shown in Fig.12. The agreement is exceptionally good throughout the range of weight coefficients for which data is available.

3.4 Sikorsky S-65 main rotor

The main rotor of the Sikorsky S-65 helicopter has been extensively tested on the firm's whirl stand. The results have been presented in Refs.3, 5 and 6 and these are supplemented by some more recent unpublished data made at higher thrust coefficients.

The main rotor of the S-65, normally known as the H53A rotor system has six blades with a radius of 11 m. The blades have a six degree twist, a chord length of 0.66 m and a modified NACA 0011 aerofoil section. The root cut out of the blades is 26% radius and the normal rotor tip speed is 213.3 m/s giving a tip Mach number of 0.626.

The data for the NACA 0011 aerofoil was obtained from Sikorsky but was only available at two Mach numbers, 0.6 and 0.7 making interpolation near the tip difficult. The aerofoil had also been tested with free transition in a wind tunnel with solid walls. A small correction has been made to the drag coefficient to make the drag level at low lift comparable to transition fixed tests but no correction has been applied to the lift coefficient although the lift curve slope of the aerofoil is rather high. Sets of data for Mach numbers

of 0.4 and 0.5 were made up based on past experience of aerofoil characteristics and the available data.

The results for the rotor presented in Ref.6 have been corrected for ground effect and whirl stand interference and a similar correction has been applied to the more recent results. The calculated performance of the rotor is compared with the experiments in Fig.13, which also shows the results predicted by strip element-momentum theory. The effect of the wake is expected to be quite large for a six bladed rotor, and Fig.13 shows that the simple theory underestimates the rotor power by between 6 and 15%. The present method is much closer to the experiments and could possibly be even better if the aerofoil data had not been so sparse. The accuracy of the whirl stand facility is quoted[5] to be ±2% of thrust at a given value of torque and the present method gives results just outside the lower bound at high thrust. No adjustments to the coordinates of the tip vortex were necessary to get this agreement whereas the tip vortex had to be moved 0.5% radius away from the blades in Ref.5. The variation of the thrust coefficient with collective pitch predicted by the theory is compared with the measurements in Fig.14. Agreement is good at low thrust but diverges as the thrust is increased. This is probably due to the high lift curve slope of the aerofoil as measured in the solid walled wind tunnel. The radial variation of the blade angle of incidence predicted by the two theoretical methods is shown in Fig.15 at a high thrust coefficient. The effect of the wake is to increase the angle of incidence at the tip by nearly 50% and the blades would obviously reach the stall much earlier than predicted by the simple theory that neglects the wake.

4 HOVER PERFORMANCE USING ONLY THE WAKE INDUCED VELOCITY DISTRIBUTION

The results presented in section 3 show that the combination of momentum theory with the wake induced velocity distribution leads to a fairly accurate and reliable calculation method, but the question remains as to why it is necessary to introduce momentum theory at all, when the wake induced velocity on its own should be sufficient to determine the rotor performance. Some of the reasons for this will be discussed in this section.

The hover performance of the Wessex main rotor measured in free flight[9] is compared with that predicted using only the wake induced velocities and the standard wake geometry in Fig.16. The Wessex rotor has been chosen because of the high quality of the experimental data and the aerofoil data for the NACA 0012 section is well defined[13]. The predicted rotor power is about 10% too great over

the complete range of thrust coefficients. The contributions to the induced and profile torque calculated with the wake induced velocities relative to those predicted by the wake momentum theory are shown in Fig.17. The induced torque is overestimated along most of the span of the blade and is mainly responsible for the poor comparison with experiment. The relative profile torque is also increased in the tip region because of the high angle of attack predicted using the wake induced velocity distribution. The blade loading predicted in the tip region for this case, which is the same as that shown in Fig.7 (Ref.11, Table 4), is 5.99 N/mm and is higher than that measured anywhere around the azimuth in the flight test.

The rotor performance predicted using the wake induced velocity is shown in Ref.5 to be very sensitive to the geometry of the wake, particularly to the vertical displacement of the tip vortex from the preceding blade. The accuracy of K_1, the relevant wake geometry parameter, is ±0.01 for a four bladed rotor which should be compared with a typical value of K_1 of 0.018 for a thrust coefficient/solidity of 0.08 and a blade with an eight degree twist. The tip vortex can therefore be moved ±1½% radius from its standard position of approximately 3½% radius and still remain within the accuracy of the model data from which the wake geometry was derived. Clearly, for the Wessex main rotor, Fig.16, there is no point in moving the tip vortex nearer to the blade as this would make the comparison even worse, and actually leads to blade stall for the whole range of thrust coefficients. The effect of increasing the magnitude of K_1 by 0.01 on the calculated rotor performance is shown in Fig.18. The comparison with experiment is now very good, perhaps slightly better than the wake momentum theory which is also shown in Fig.18. Other examples have been calculated, though the results are not shown here, which demonstrate the same features as the Wessex, that the power is always overestimated when the tip vortex is in its standard position but the agreement with experiment can be improved if the tip vortex from the preceding blade is displaced further from the rotor disc. The change in rotor power due to moving the tip vortex can be very large; for the Wessex a change in the displacement of the tip vortex by ±1½% radius leads to a variation in power of about +20% to -10%, and for this reason a calculation based solely on the wake induced velocity distribution cannot be used as a design tool with any confidence.

A change in the displacement of the tip vortex below the rotor disc using the wake induced velocities alone produces a change in the integrated induced

velocity and hence to the momentum through the disc. This of course leads to changes in the predicted power and the shape of the radial load distribution. Introducing the wake induced velocity as a perturbation to the momentum downwash and ensuring that the thrust on each element of the blade using strip element theory is consistent with momentum theory appears to reduce the sensitivity to tip vortex location considerably and to keep changes in the radial load distribution to a minimum.

The variation of rotor performance with changes in the rotor geometry is to be expected as both model and full scale tests generally show a scatter in the power required to produce a given thrust, but the observed variation is much smaller than that predicted using the wake induced velocities. The wake in its standard position, as used throughout section 3, would be expected to give a reasonable approximation to the mean performance of the rotor, whereas in all the cases considered, the rotor power was overestimated and the tip vortex has had to be moved further away from the blade. This suggests that the representation of the wake, and in particular, the tip vortex by a series of trailing line vortex elements is inadequate. Cook[16] has investigated the structure of the tip vortex from a rotor blade using a hot wire anemometer and has shown that the effective size of the vortex core was larger than simple theory suggested although the vortex core was significantly smaller. The velocity field induced by the tip vortex was also considerably different from that represented by a vortex with uniform vorticity in the core. The mathematical representation of the tip vortex, and possibly the rest of the wake would seem to be oversimplified and this may be the reason why some of the 'free wake' methods as well as the prescribed wake methods fail to achieve the expected results. The wake momentum theory appears to overcome these problems by its treatment of the wake velocity as an interference velocity and leads to a more reliable calculation.

5 CONCLUSIONS

A method of predicting the performance of a helicopter rotor in the hover has been developed. The calculation combines strip element-momentum theory with the inflow distribution induced by a contracting vortex wake. The wake takes a prescribed geometry developed from a comprehensive series of model tests made in the USA.

The theory has been compared with measurements made on model and full scale rotors and has always predicted the rotor thrust and power accurately

provided that the two-dimensional aerofoil data is adequately defined. The calculated blade load distribution has also been compared with measurements made on two Wessex helicopters. The comparison with the time averaged measurements is confused because the geometry of two of the helicopter blades was different, and the effect of a light wind could only be estimated but the radial position of the peak load was correctly predicted. The other comparison showed good agreement between theory and experiment because the azimuthal variation of the blade load was known, and the effect of the wind could be eliminated to a certain extent.

These comparisons highlighted several aspects of hovering flight in the real environment. The effect of a light wind may have a negligible influence on the power required to produce a given thrust, but may have a significant effect on the blade load distribution and wake stability. The blade load near the tip is increased over a greater part of the disc, and may lead to premature blade stall. This has important consequences for the helicopter designer who must provide an adequate margin between the lift coefficient predicted near the tip in ideal hover and the aerofoil separation boundary. This is especially true of tail rotors which can also suffer a large loss of usable thrust due to fin blockage and the main rotor wake affecting the forces on the tail boom and fin.

The wake geometry employed in the present method is only applicable for untapered, rectangular tipped blades operating within a certain range of parameters. Small excursions outside the range of conditions on which the wake model was based seem permissible but a new wake geometry will almost certainly be required for blades with complex tip shapes.

The rotor performance predicted using only the wake induced velocity distribution has been compared with experimental results for the main rotor of a Wessex helicopter. Agreement with experiment was only possible if the tip vortex from the preceding blade was displaced further below the plane of the disc than indicated by the standard wake geometry although the displacement required was within the accuracy of the experimental data on which the wake was based. However, it is believed that there are other fundamental difficulties in using the wake induced velocities which only a better understanding of the real flow would resolve. There is still plenty of scope for workers in this field to find a satisfactory solution to the problem of predicting rotor hover performance.

Acknowledgment

The author wishes to thank Westland Helicopters Ltd. for the helpful discussions had during the course of this work.

SYMBOLS

a_0	blade coning angle
b	number of blades
c	blade chord
c_i	blade chord distribution
c_q	torque coefficient, $c_q = Q/\pi\rho R^5\Omega^2$
c_T	thrust coefficient, $c_T = T/\pi\rho R^4\Omega^2$
c_w	weight coefficient, $c_w = W/\pi\rho R^4\Omega^2$
e	flap hinge offset
g	acceleration due to gravity
I_b	second moment of inertia of blade about flapping hinge
K_1, K_2	wake geometry coefficients
K_{11}, K_{21}, K_{20}	wake geometry coefficients
M_A	aerodynamic moment about the flapping hinge
M_b	first moment of inertia of blade about flapping hinge
Q	total rotor torque
Q_i	blade torque distribution
r	radial coordinate
$\bar{r}$	non-dimensional radial coordinate, $\bar{r} = r/R$
r_i	radial position defining the ends of the blade elements
$\bar{r}_i$	mid points of blade elements
R	rotor radius
s	rotor solidity ratio, $s = bc/\pi R$
T	total rotor thrust
T_i	blade thrust distribution
u_i	total downwash velocity distribution, $u_i = -(Y_i + w_i)$
W	aircraft weight
w_i	momentum part of downwash velocity distribution
Y_i	wake interference velocity distribution
z	vertical coordinate
$\bar{z}$	non-dimensional vertical coordinate, $\bar{z} = z/R$

SYMBOLS (concluded)

α_i	blade incidence distribution
β_i	wake interference angle, $\beta_i = \tan^{-1} (Y_i/\Omega\bar{r}_i)$
γ_i	trailing vortex strength
Γ_i	bound vortex strength
$\partial C_L/\partial\alpha$	aerofoil lift curve slope
η_i	initial inflow angle $\eta_i = \tan^{-1} (v_1/\Omega\bar{r}_i)$
θ_1	blade linear twist
θ_i	blade twist distribution
θ_R	blade collective pitch
λ	wake geometry coefficient
v_i	initial momentum downwash distribution
ρ	air density
σ_{ij}	wake induced velocity influence coefficient
ϕ_i	momentum inflow angle, $\phi_i = \tan^{-1} (w_i/\Omega\bar{r}_i)$
ψ	azimuth angle
ψ_b	azimuth separation of blades
Ω	rotor rotational speed

REFERENCES

No.	Author	Title, etc.
1	H.H. Pearcey P.G. Wilby M.J. Riley P. Brotherhood	The derivation and verification of a new rotor profile on the basis of flow phenomena, aerofoil research and flight tests. Paper 16 in The aerodynamics of rotary wings, AGARD CP 111 (1972)
2	W.Z. Stephniewski	Basic aerodynamics and performance of the helicopter. Paper 2 in Helicopter aerodynamics and dynamics, AGARD LS 63 (1973)
3	D.R. Clarke A.C. Leiper	The free wake analysis - a method for the prediction of helicopter rotor hovering performance. Journ. American Helicopter Soc., 15, No.1, 3-11, (1970)
4	A.J. Landgrebe	An analytical method for predicting rotor wake geometry. Journ. American Helicopter Soc., 14, No.4, 20-32, (1969)
5	A.J. Landgrebe	An analytical and experimental investigation of helicopter rotor hover performance and wake geometry characteristics. USA AMRDL Technical Report 71-24 (1971)
6	J.B. Rorke C.D. Wells	The prescribed wake momentum analysis. Proceedings of the 3rd CAL/AVLABS Symposium on Aerodynamics of rotary wings and V/STOL aircraft, Vol.1, Cornell Aeronautical Lab Inc., Buffalo, New York, June 1969
7	J.L. Tangler R.M. Wohlfeld S.J. Miley	An experimental investigation of vortex stability, tip shapes, compressibility and noise for hovering model rotors. NASA CR 2305 (1973)
8	R.A. Piziali F.A. Du Waldt	A method of computing rotary wing airload distribution in forward flight. CAL Report BB-1495-S-1 (1962)
9	P. Brotherhood D.W. Brown	RAE Technical Report to be published.

REFERENCES (concluded)

No.	Author	Title, etc.
10	M.J. Riley P. Brotherhood	Comparative performance measurements of two helicopter blade profiles in hovering flight. RAE Technical Report 74008 (ARC 35289) (1974)
11	J. Scheiman	A tabulation of helicopter blade differential pressures, stresses, and motions as measured in flight. NASA TM-X 952 (1964)
12	A.R. Mettam R.J. Marshall	24ft tunnel tests of a Wessex tail rotor with variable fin blockage. RAE Technical Memorandum Aero 1028 (1967)
13	N. Gregory P.G. Wilby	NPL 9615 and NACA 0012. A comparison of aerodynamic data. ARC CP 1261 (1973)
14	C.V. Cook	Rotor performance prediction in hover. Westland Helicopters Ltd., Research Paper 357 (1968)
15	P.G. Wilby	Effect of production modifications to rear of Westland Lynx rotor blade on sectional aerodynamic characteristics. RAE Technical Report 73043 (ARC 34835) (1973)
16	C.V. Cook	The structure of the rotor blade tip vortex. Paper 3 in The aerodynamics of rotary wings, AGARD CP 111 (1972)

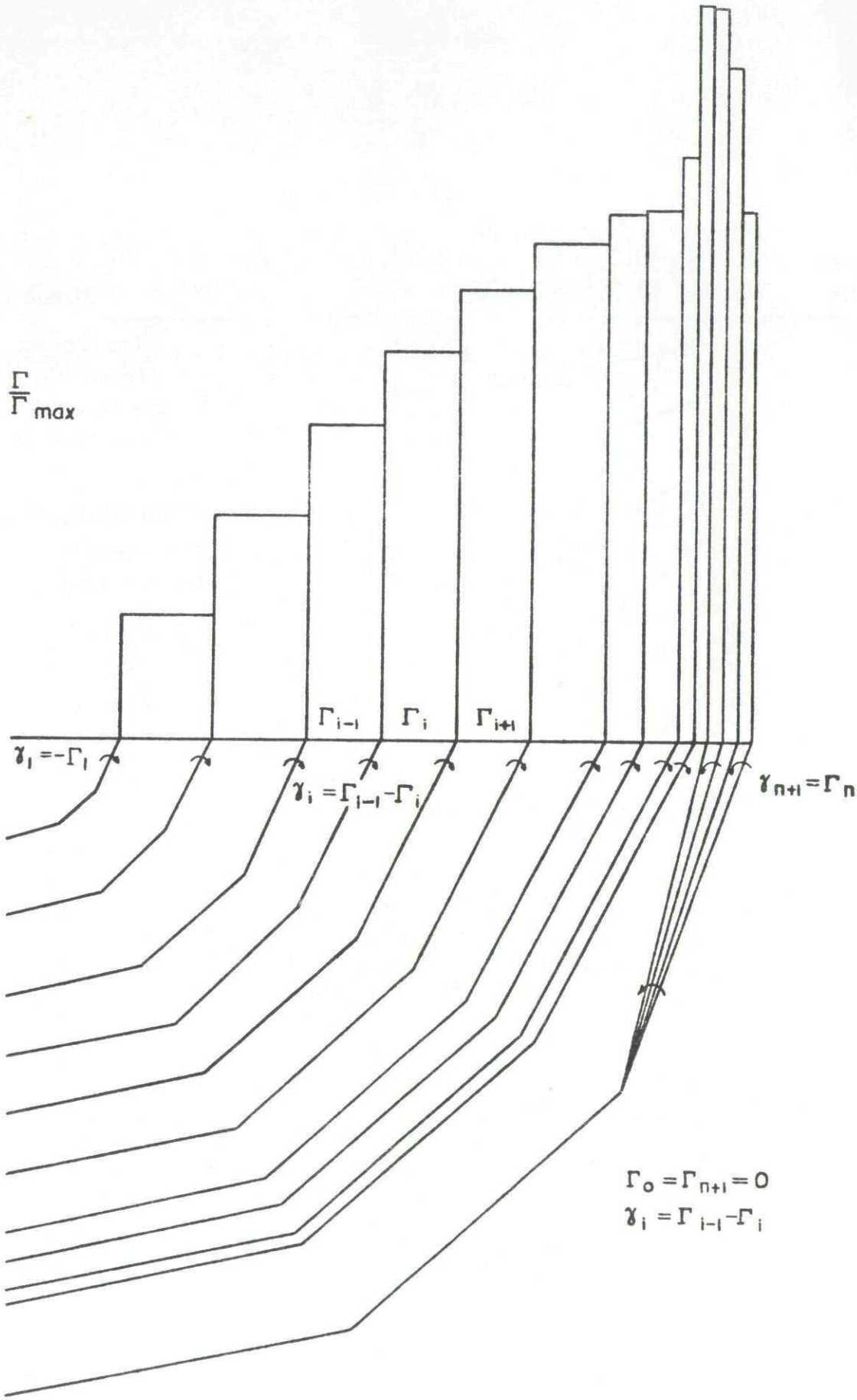

Fig.1 Bound and trailing vortex strength distributions and initial wake

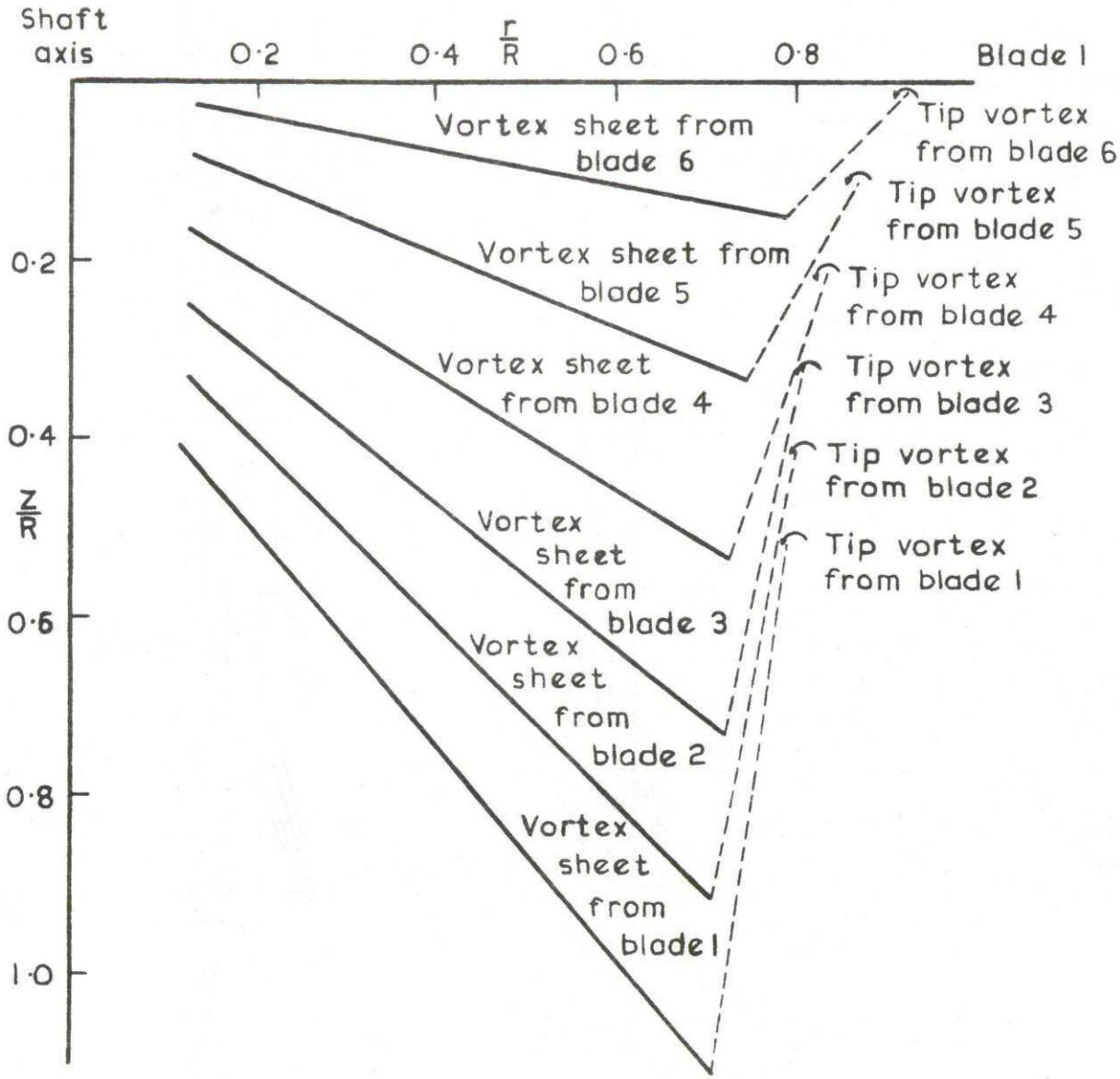

Fig. 2 Cross section of one revolution of the wake from a six bladed rotor

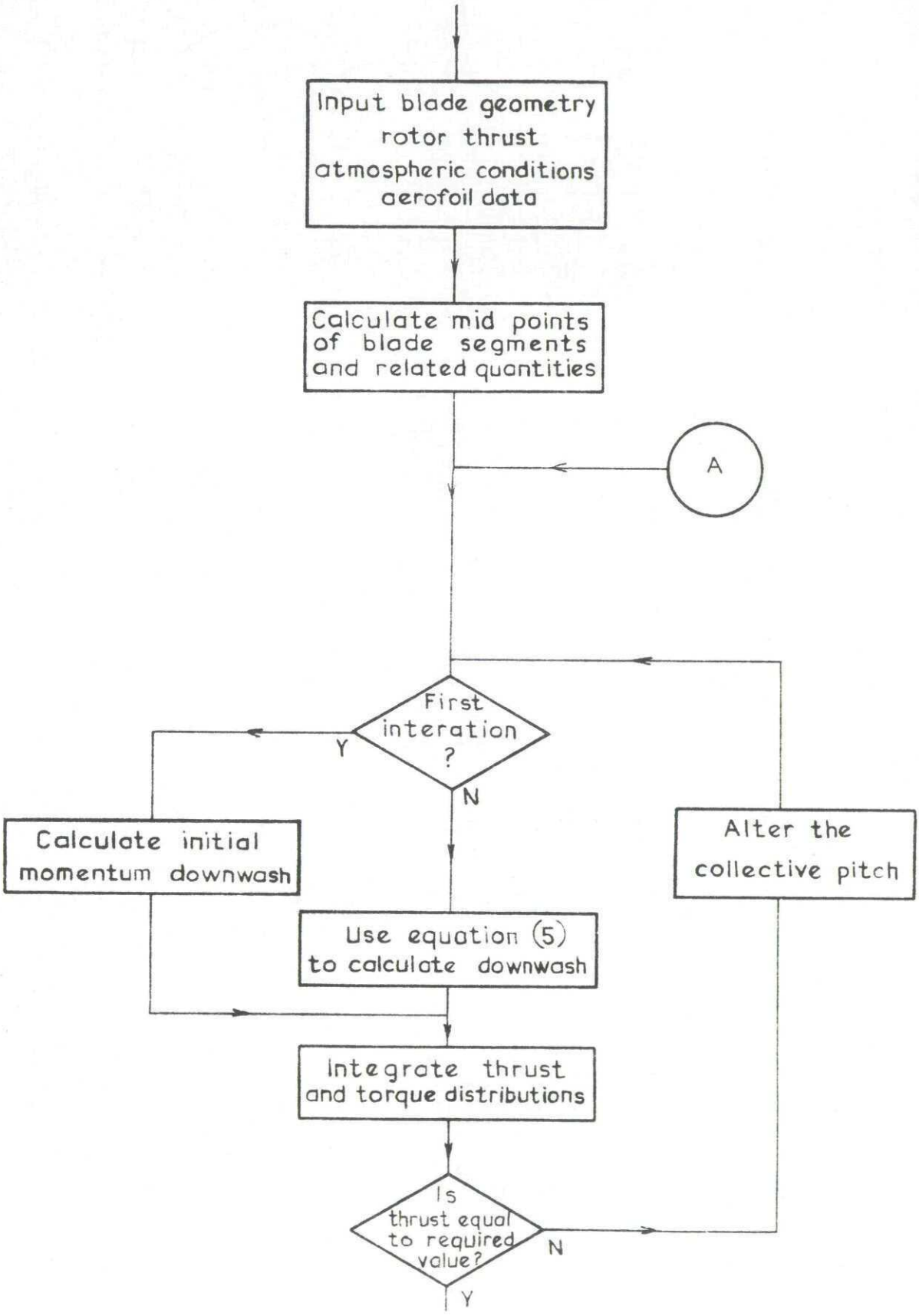

Fig.3 Flow diagram of the performance calculation

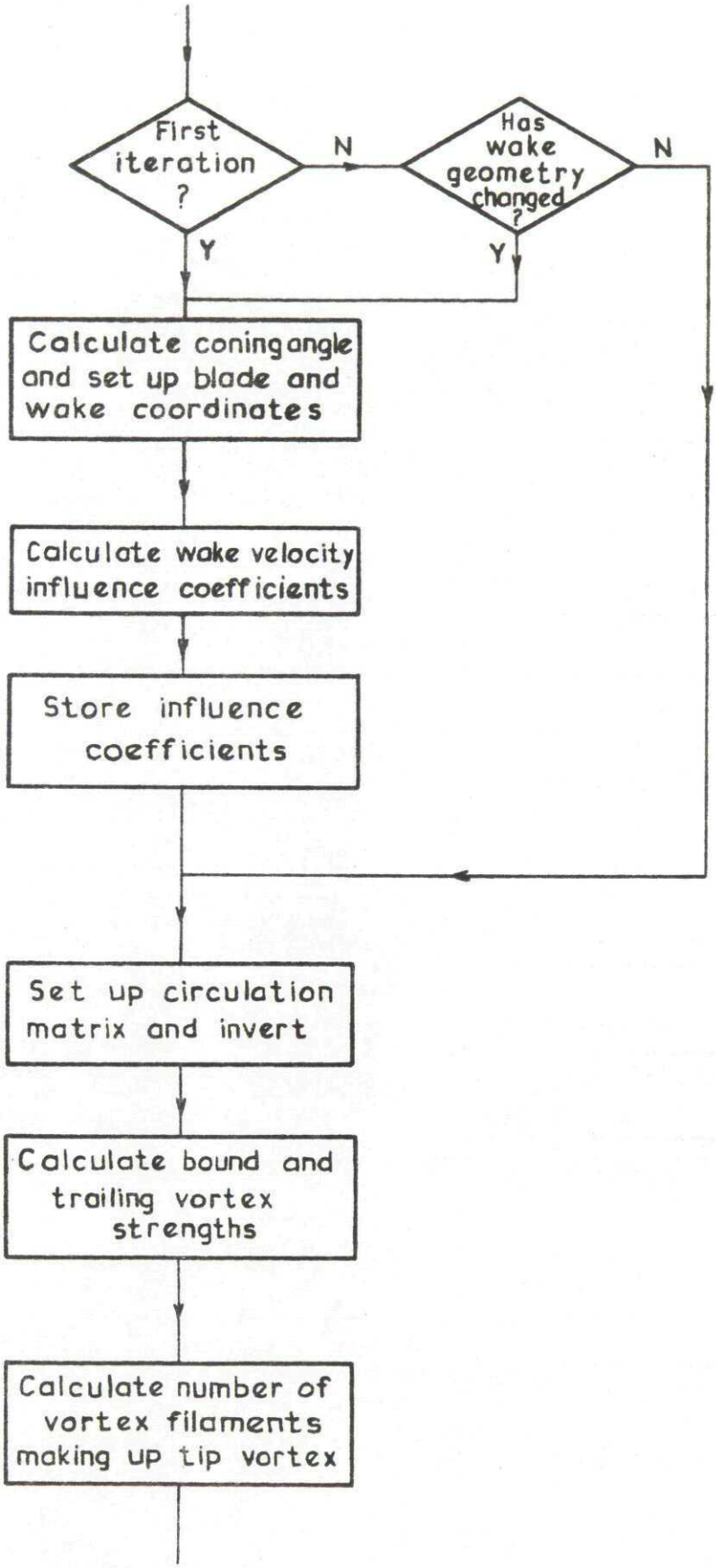

Fig.3 contd Flow diagram of the performance calculation

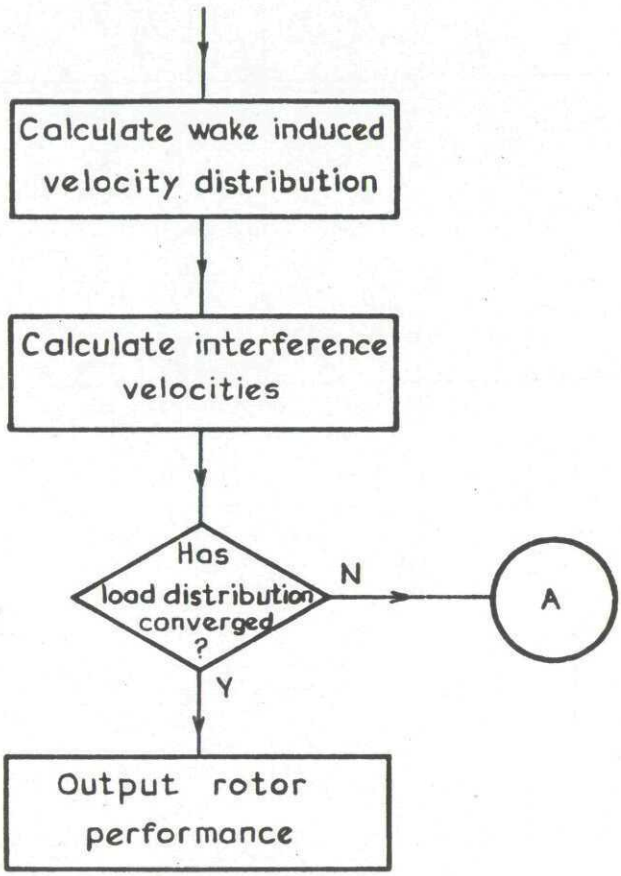

Fig.3 concld Flow diagram of the performance calculation

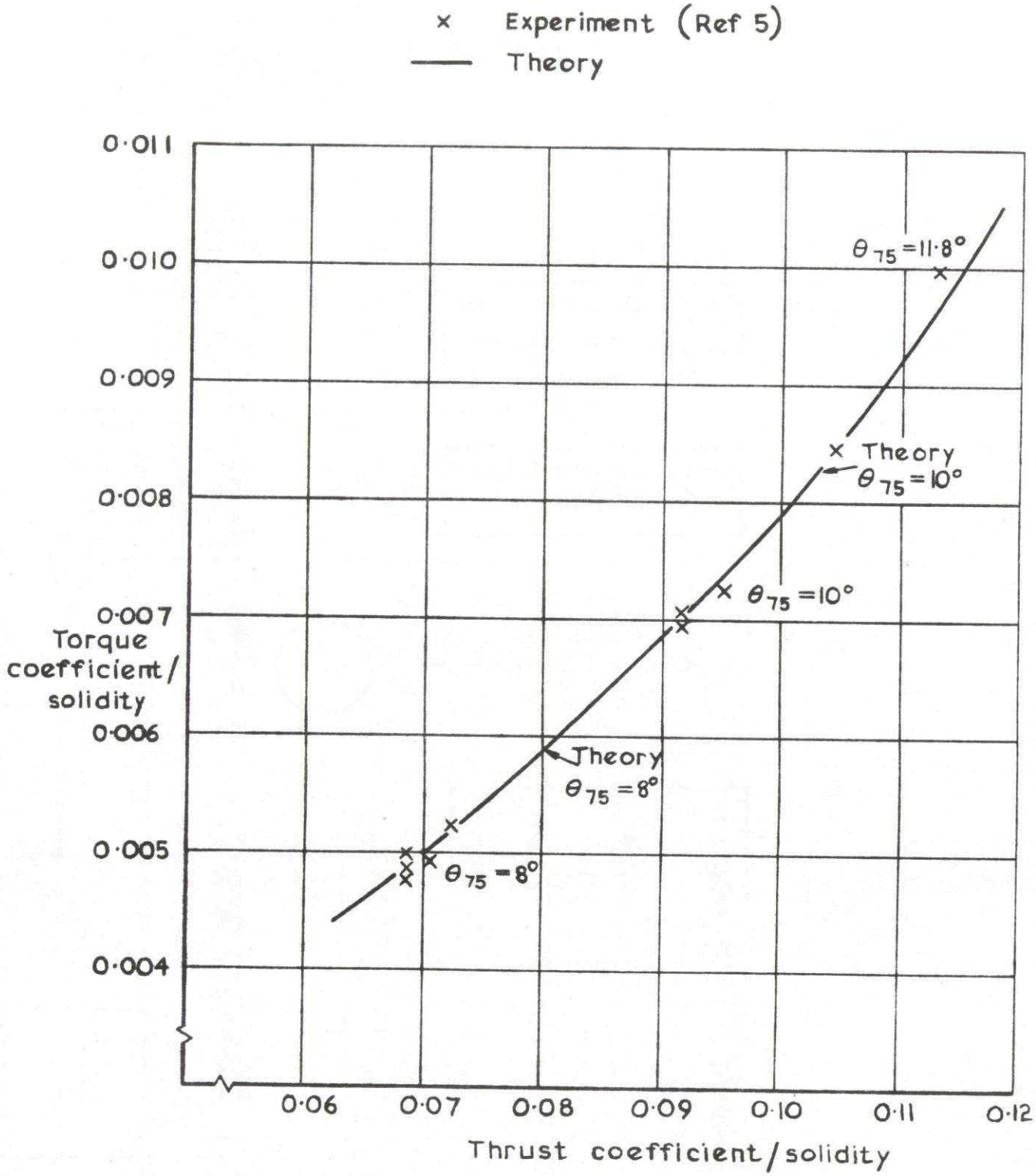

Fig. 4 Measured and predicted thrust and torque coefficient for a two bladed model rotor

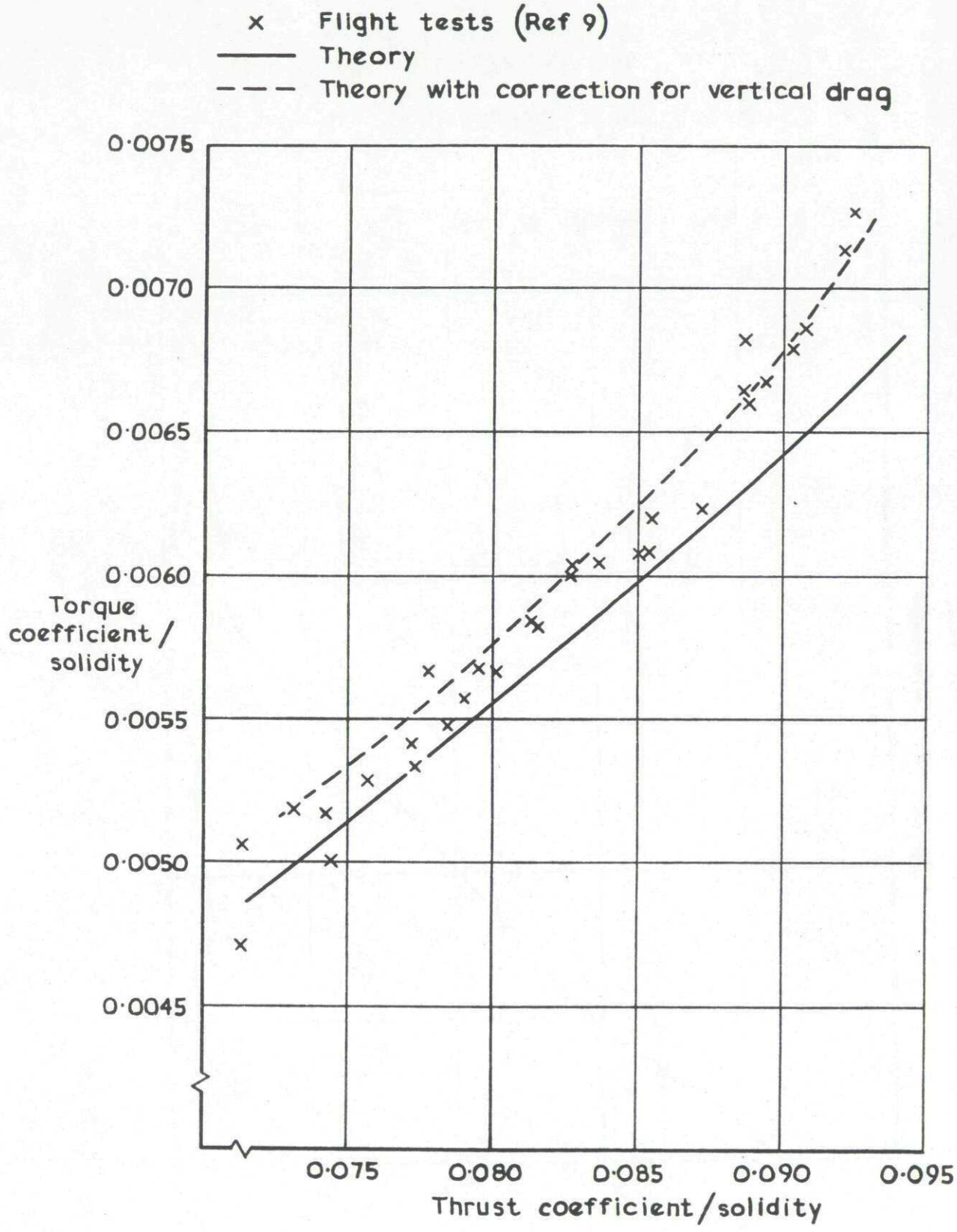

Fig.5 Wessex main rotor thrust and torque coefficients

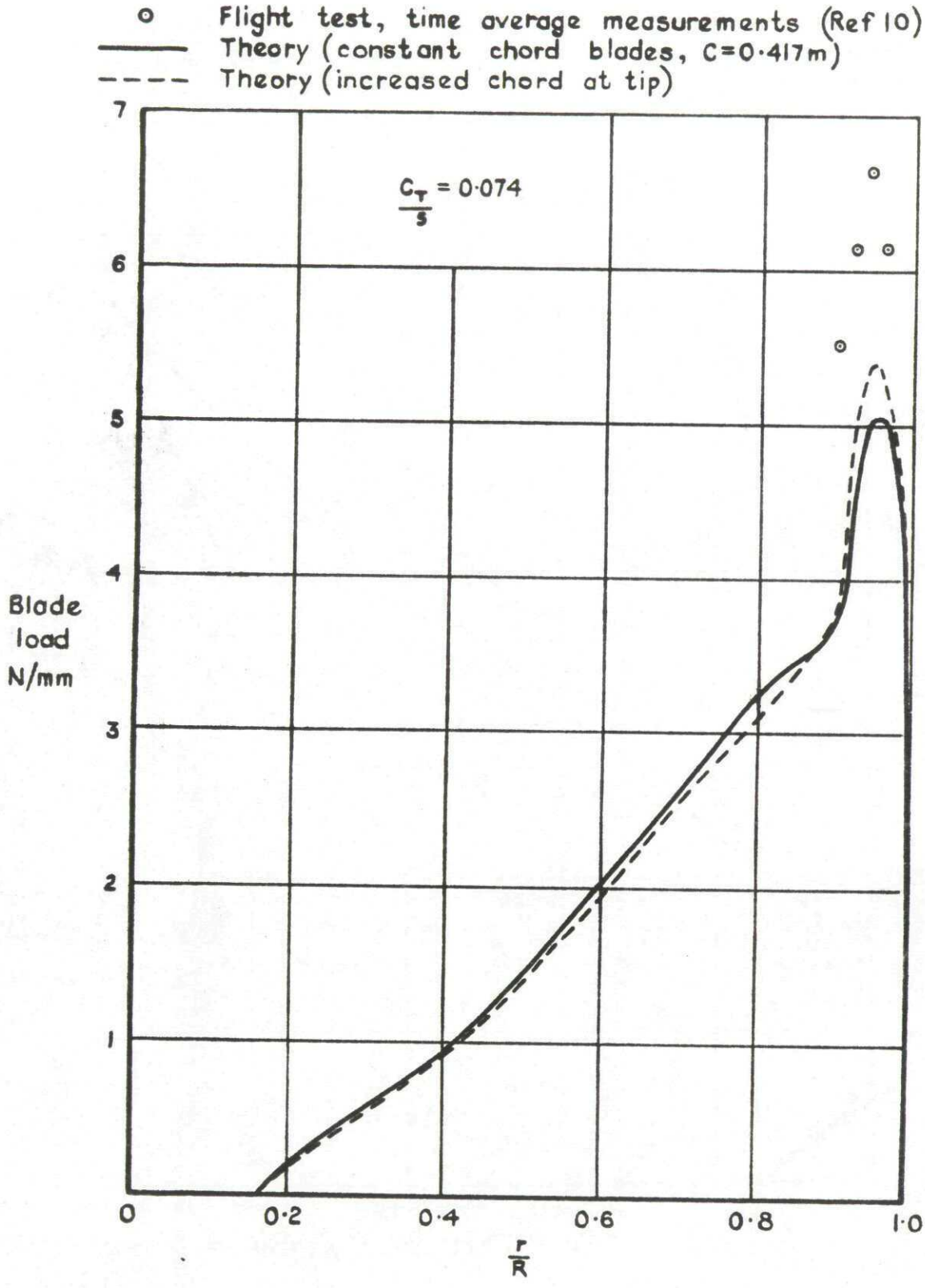

Fig. 6 Measured and predicted radial load distribution for a Wessex main rotor

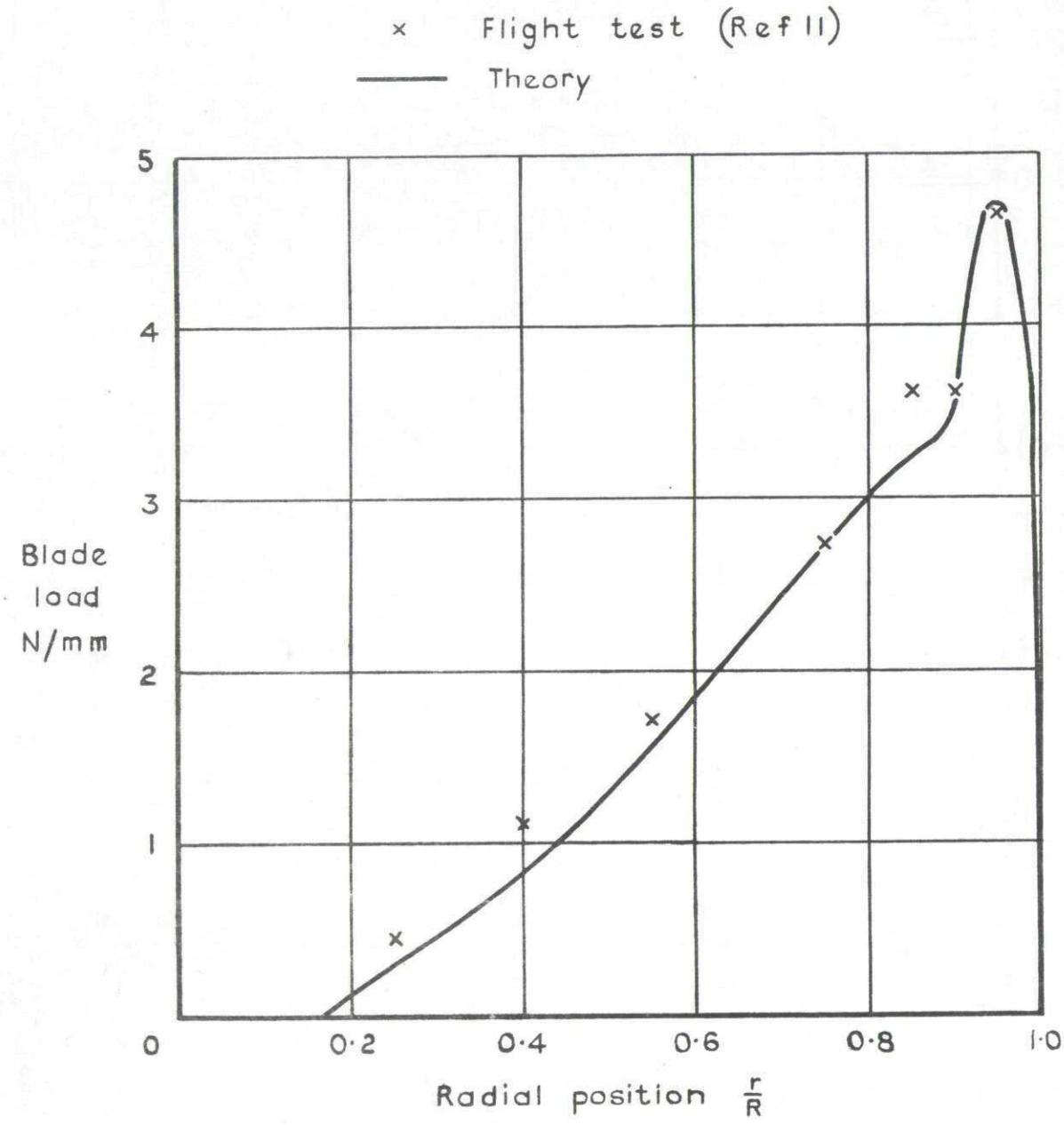

Fig. 7 Measured and predicted radial load distribution for a Wessex main rotor

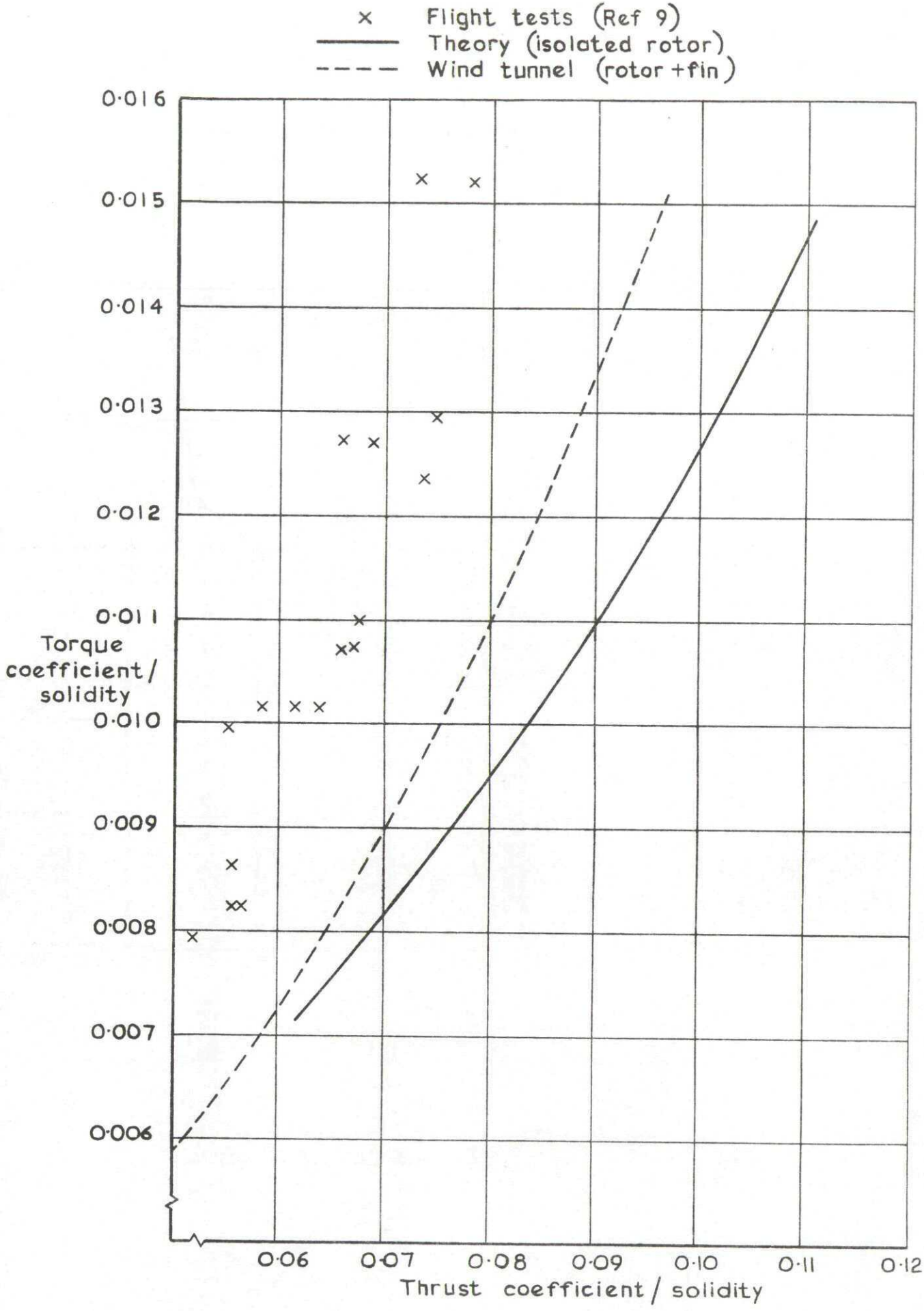

Fig. 8 Wessex tail rotor thrust and torque coefficients from wind tunnel, flight tests and theory

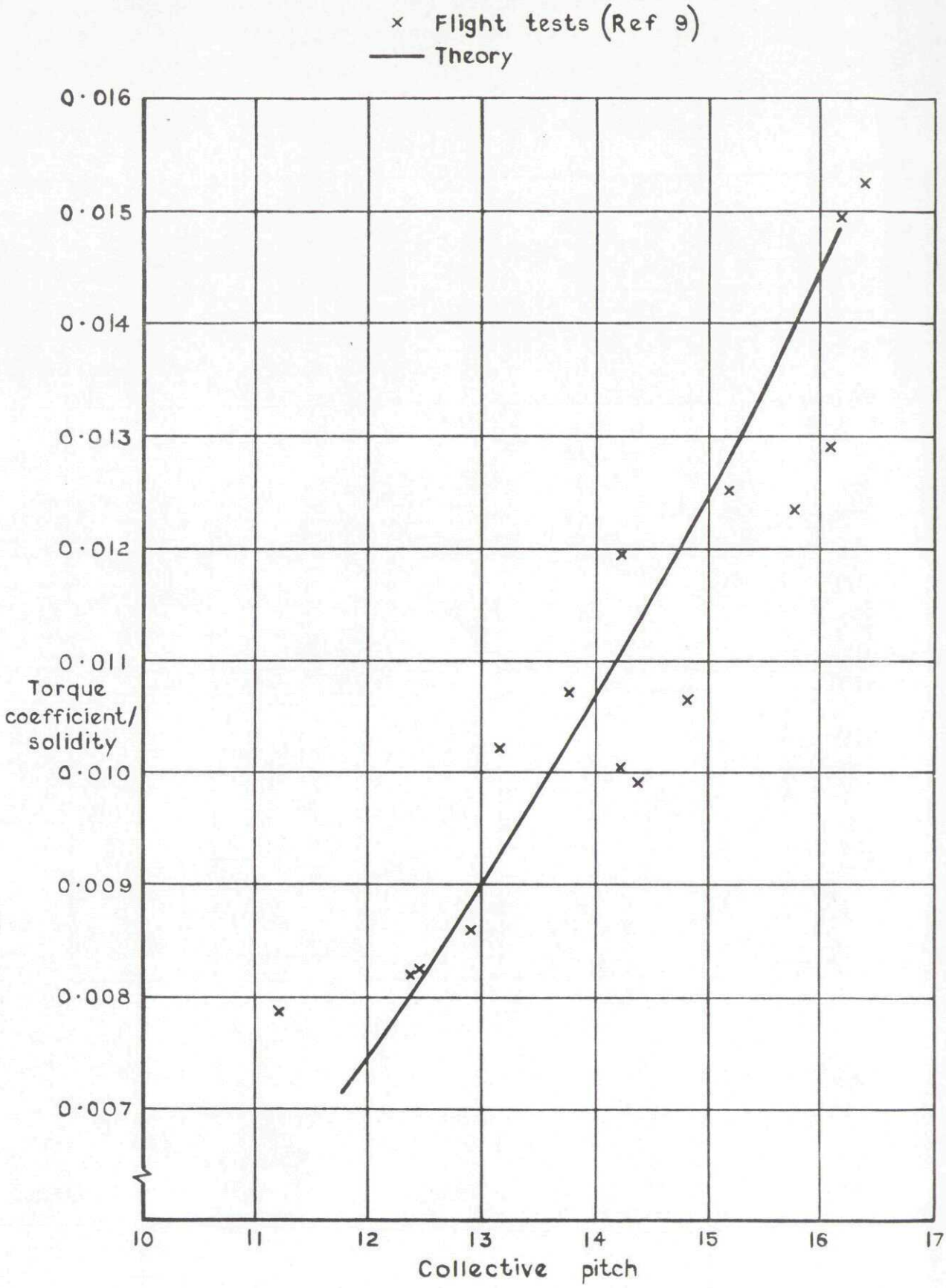

Fig. 9 Measured and calculated collective pitch for Wessex tail rotor

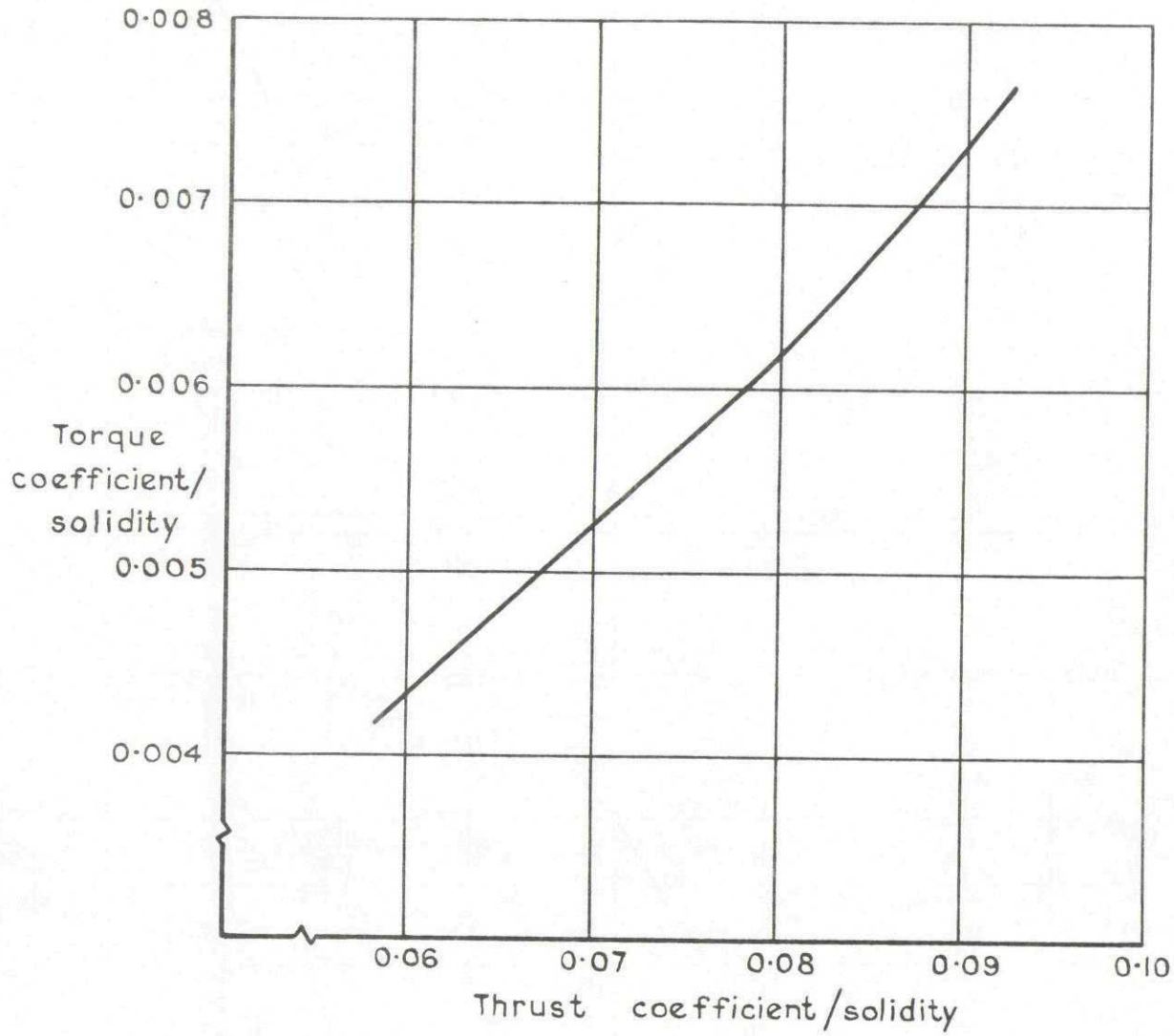

Fig. 10 Predicted thrust and torque coefficient for the Sea King main rotor

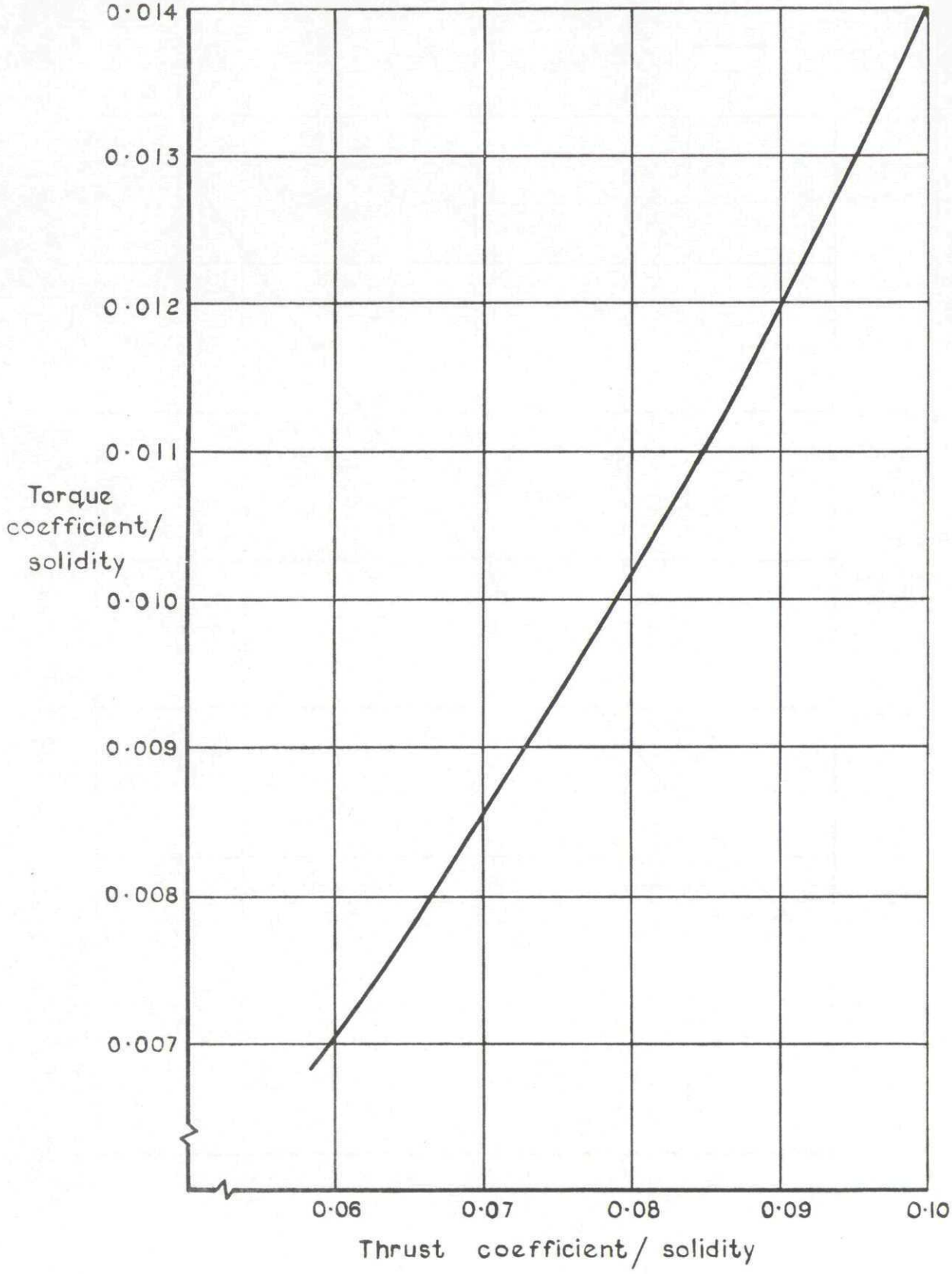

Fig. 11 Predicted thrust and torque coefficient for the Sea King tail rotor

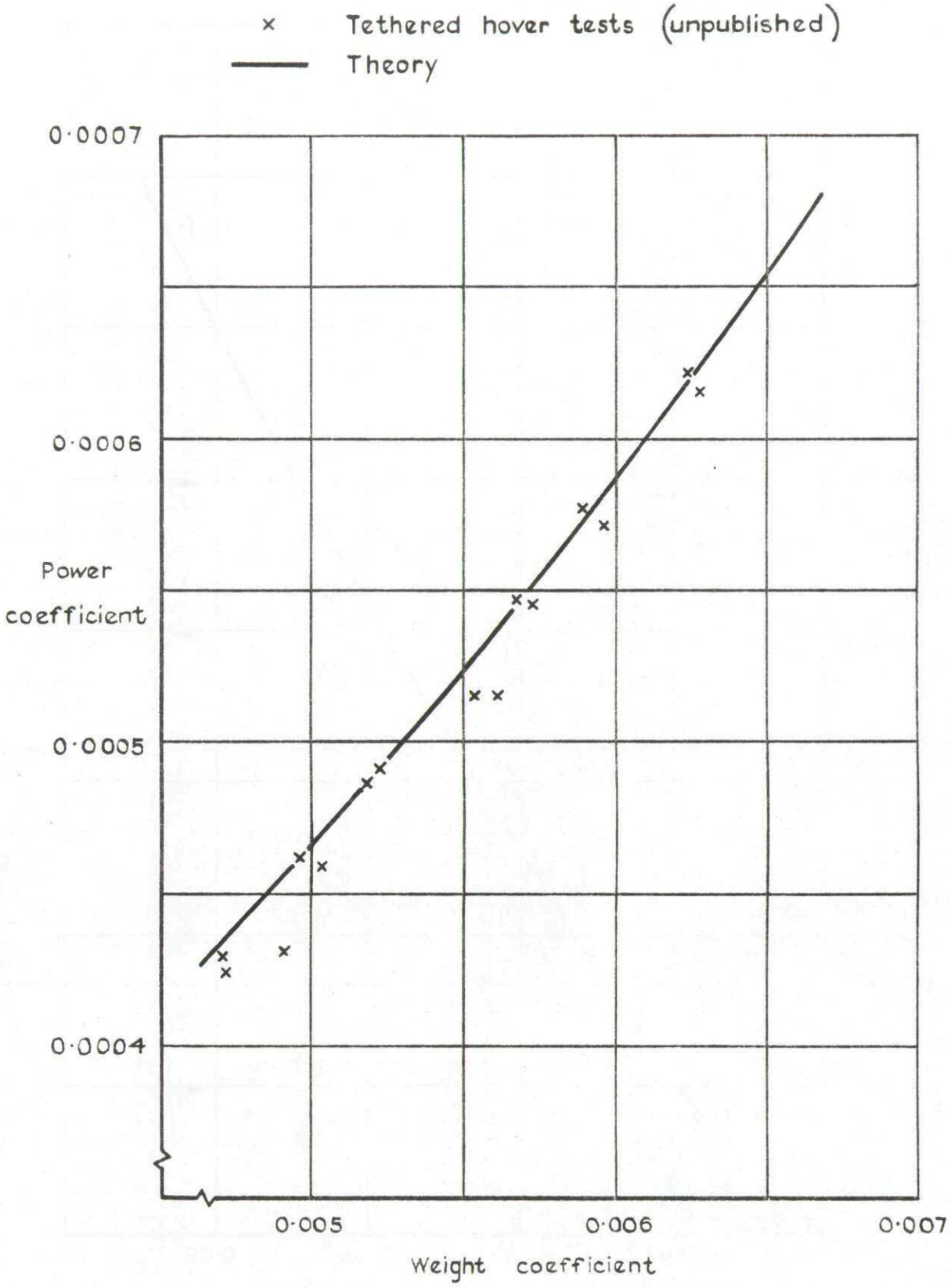

Fig. 12 Measured and predicted hover performance for the Sea King

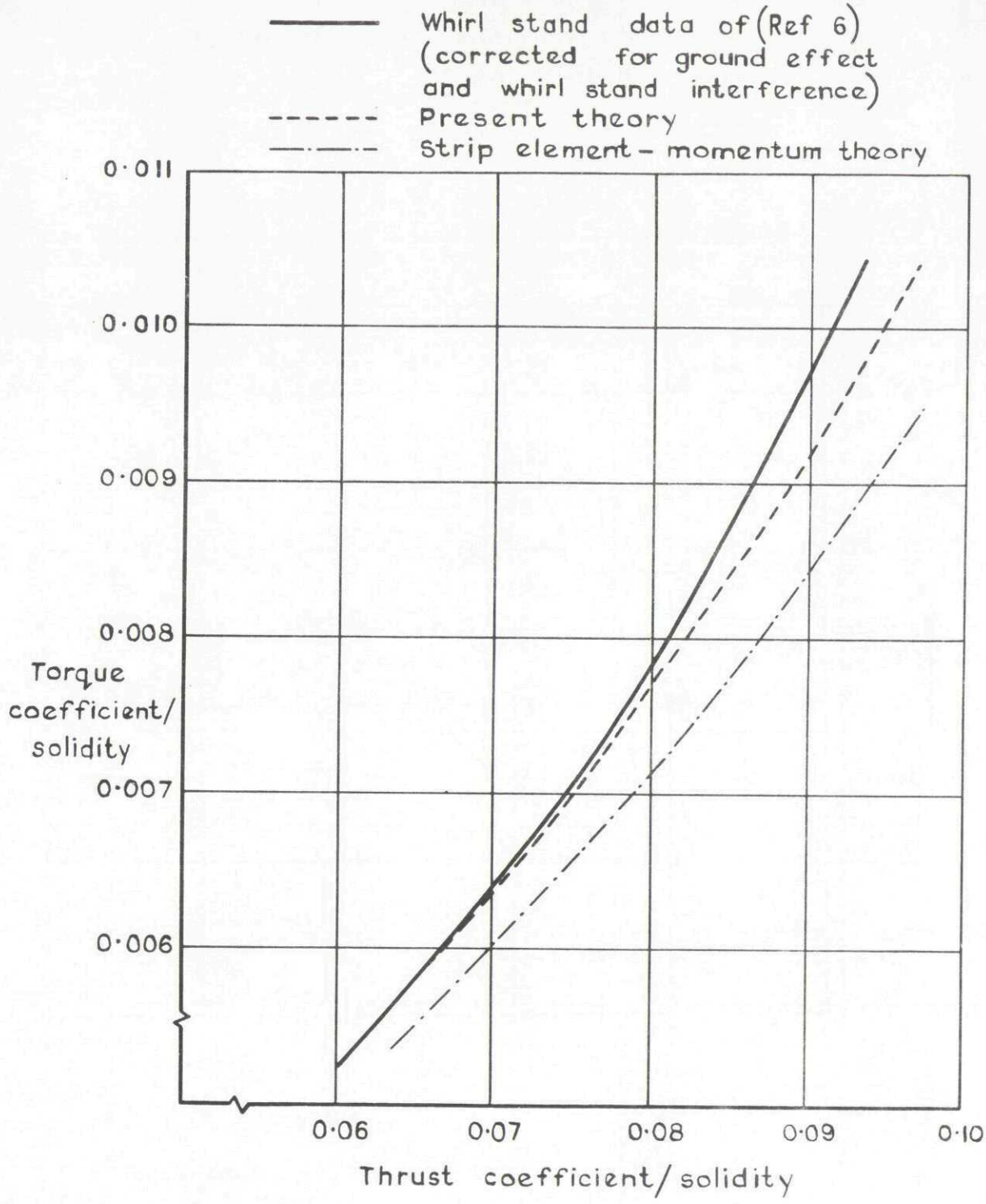

Fig. 13 Predicted and measured thrust and torque coefficients for CH 53 A rotor

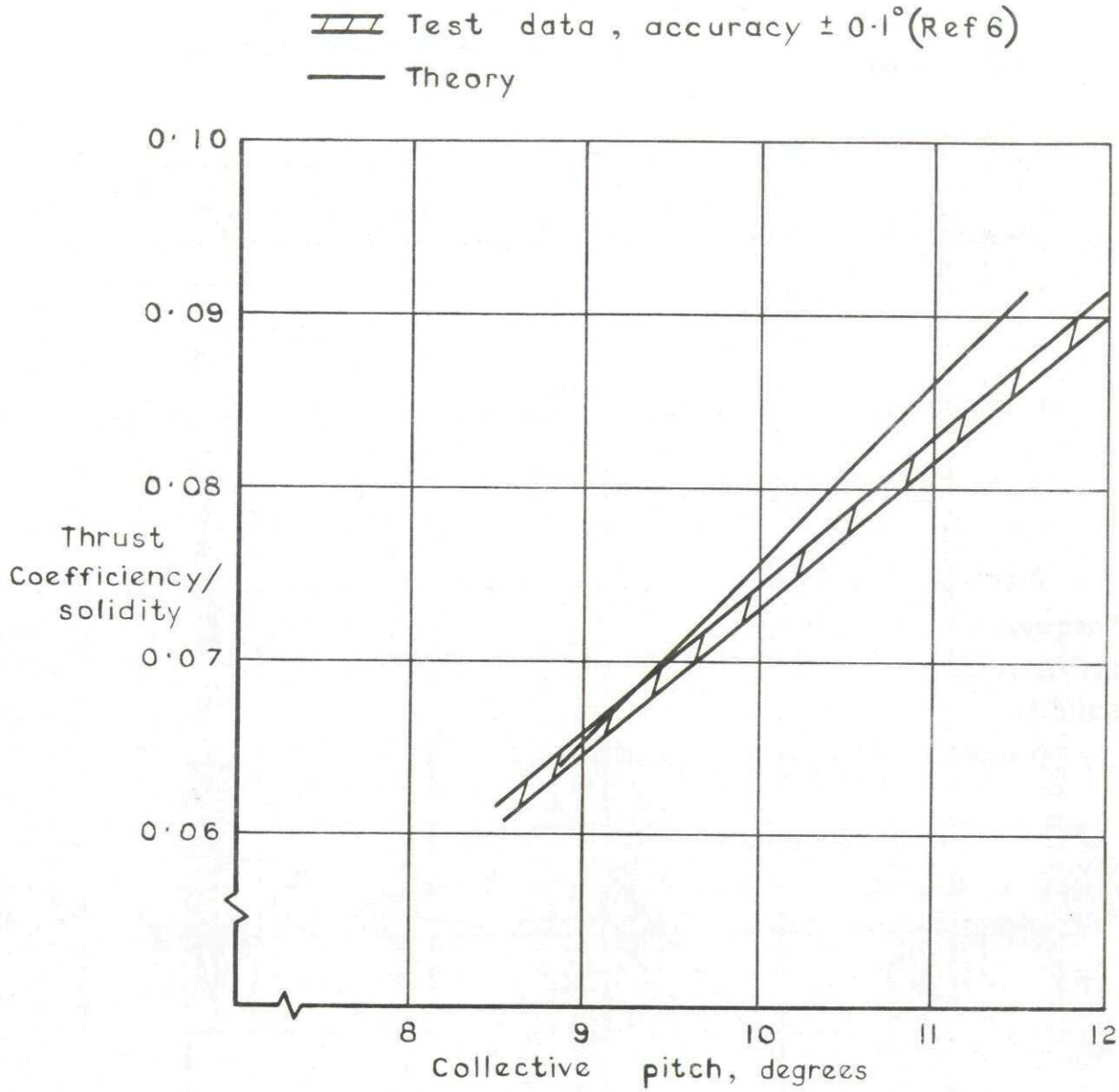

Fig. 14 Rotor thrust coefficient and collective pitch for CH 53A rotor

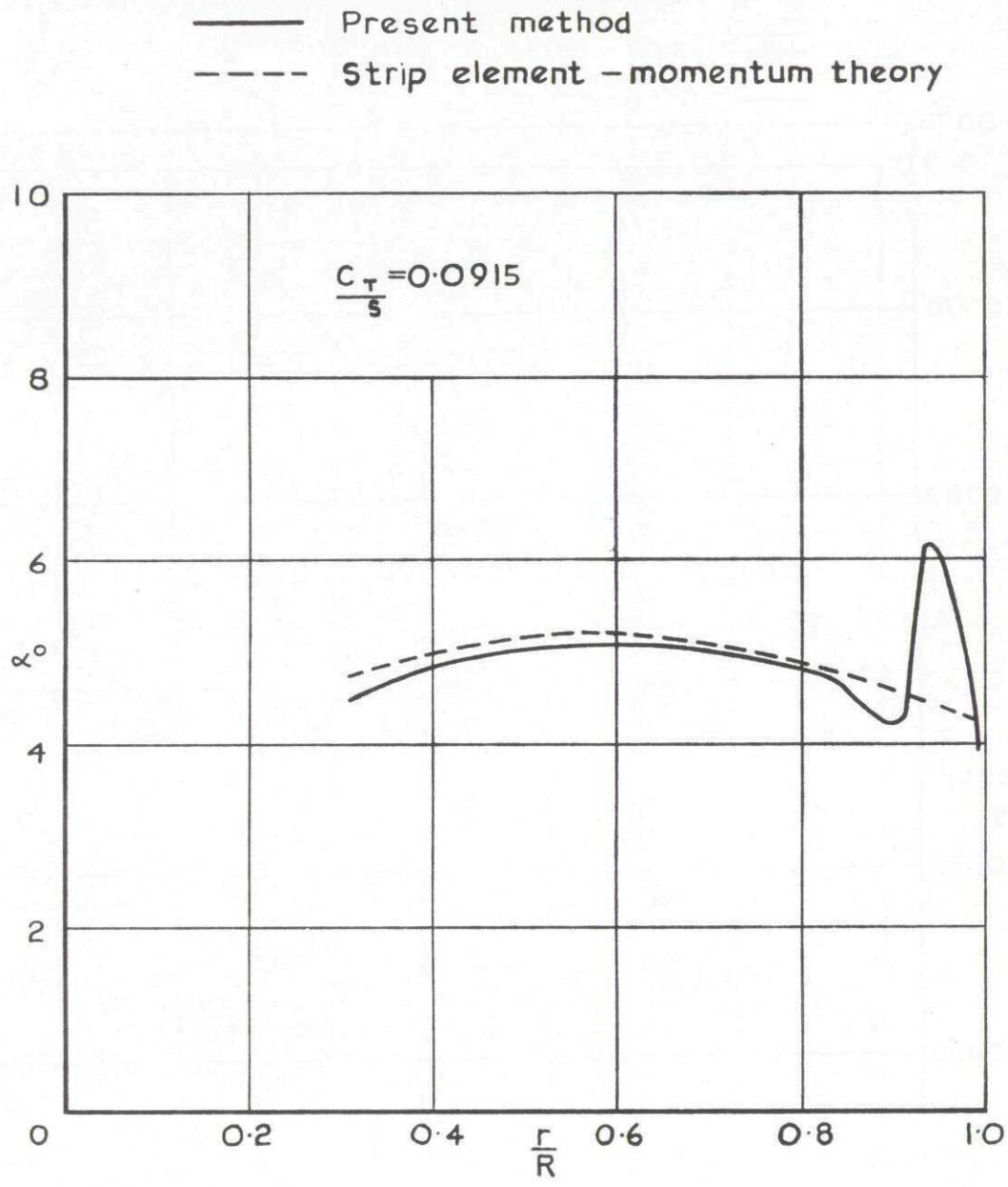

Fig.15 Blade angle of incidence distribution for six bladed CH 53 rotor

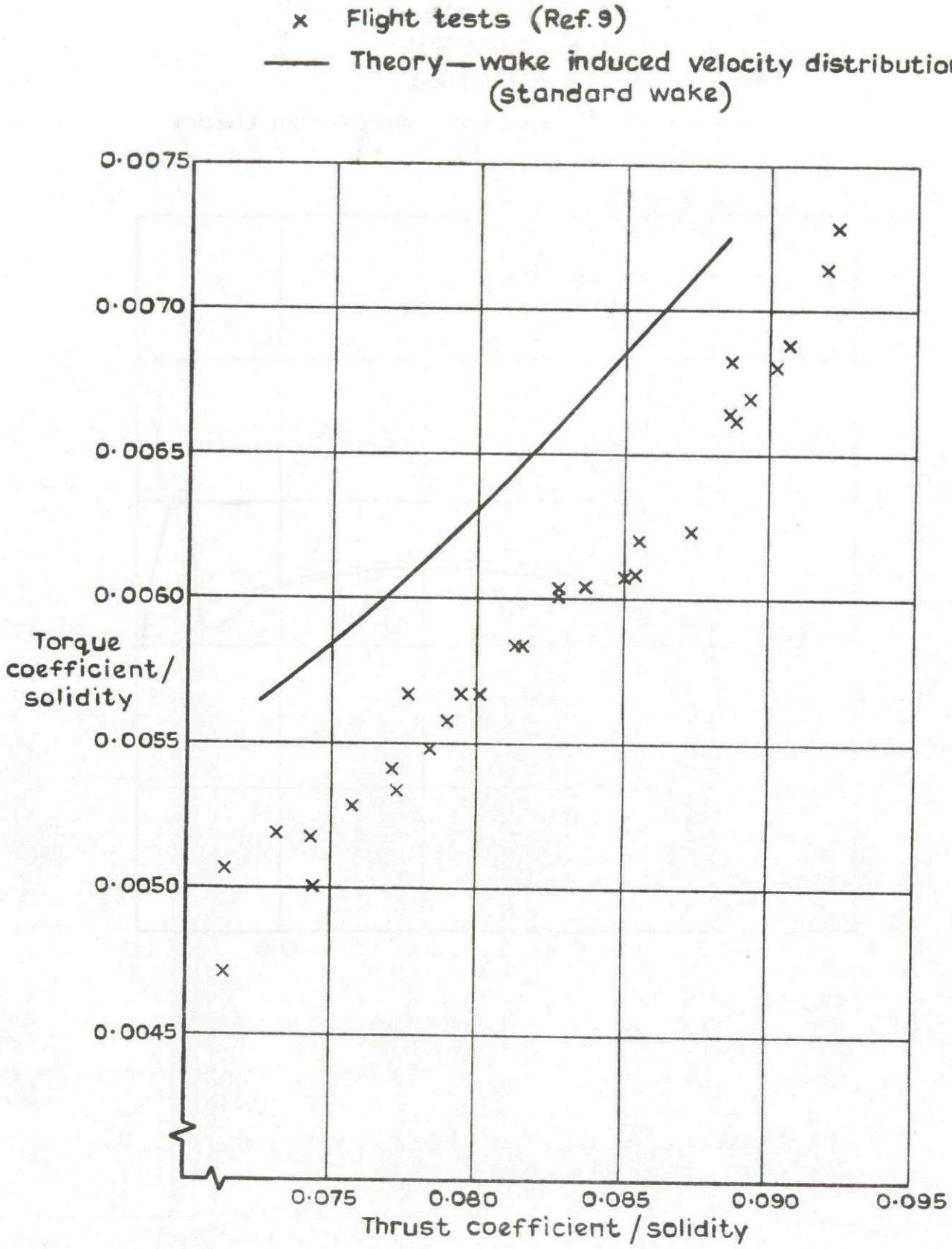

Fig. 16 Wessex main rotor performance, experiment and theory using wake induced velocity distribution

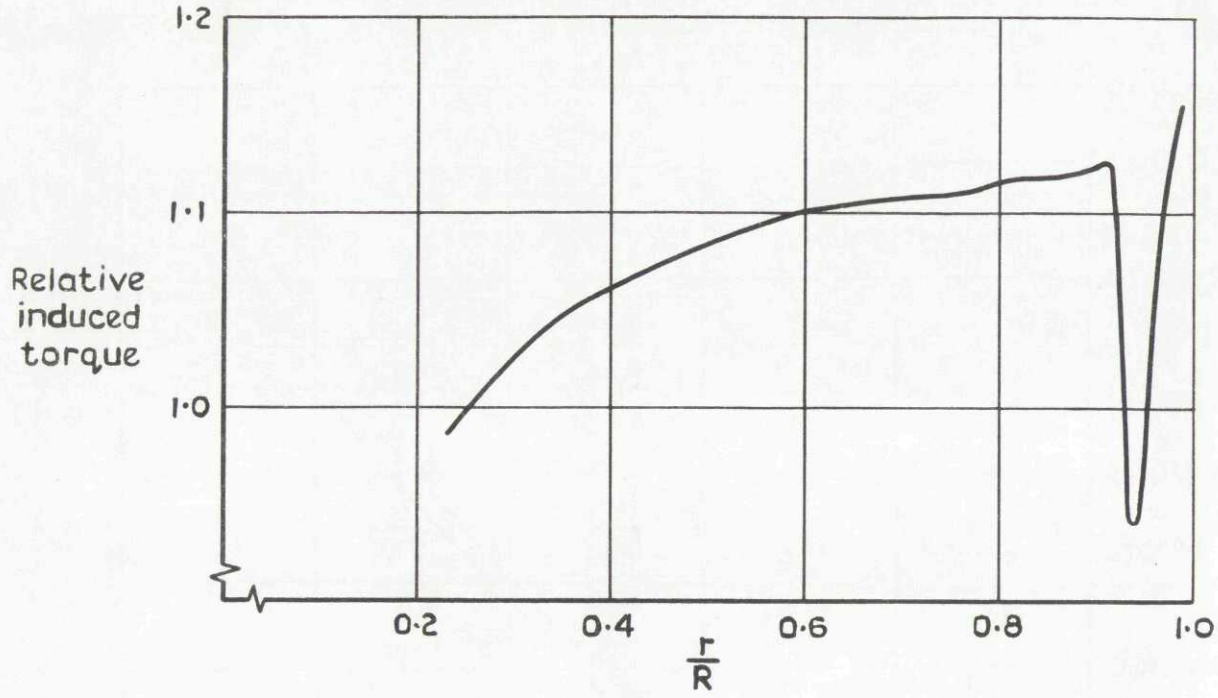

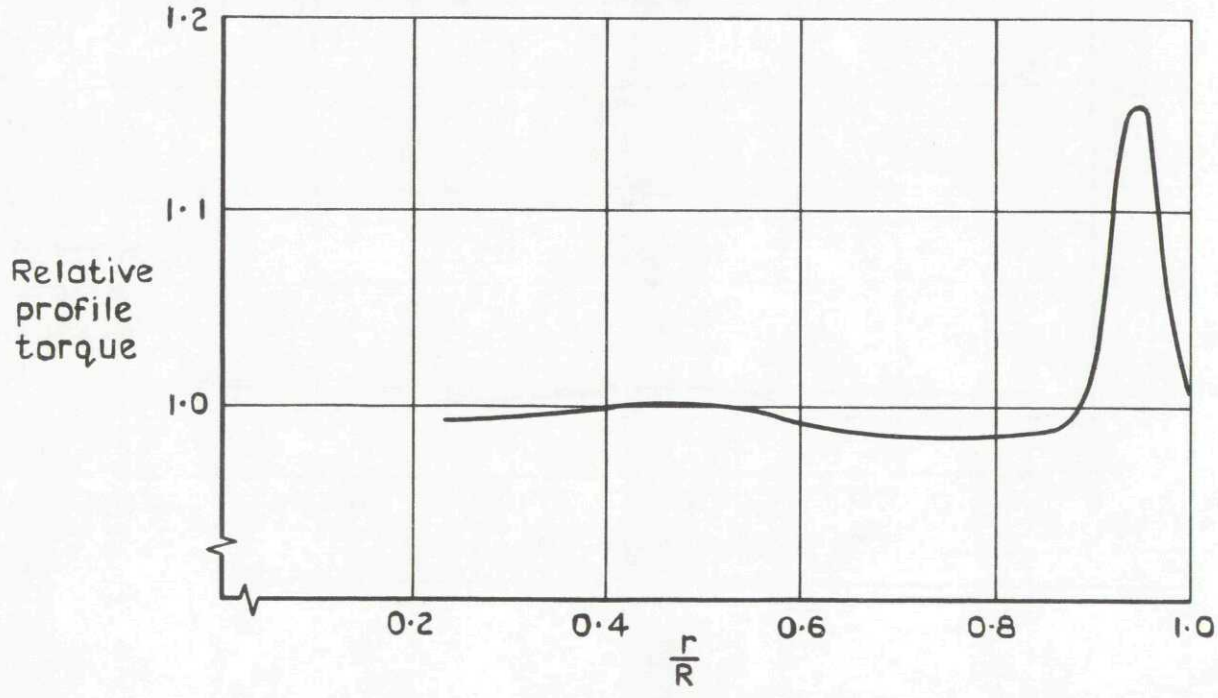

Fig.17 Relative torque distributions for Wessex main rotor

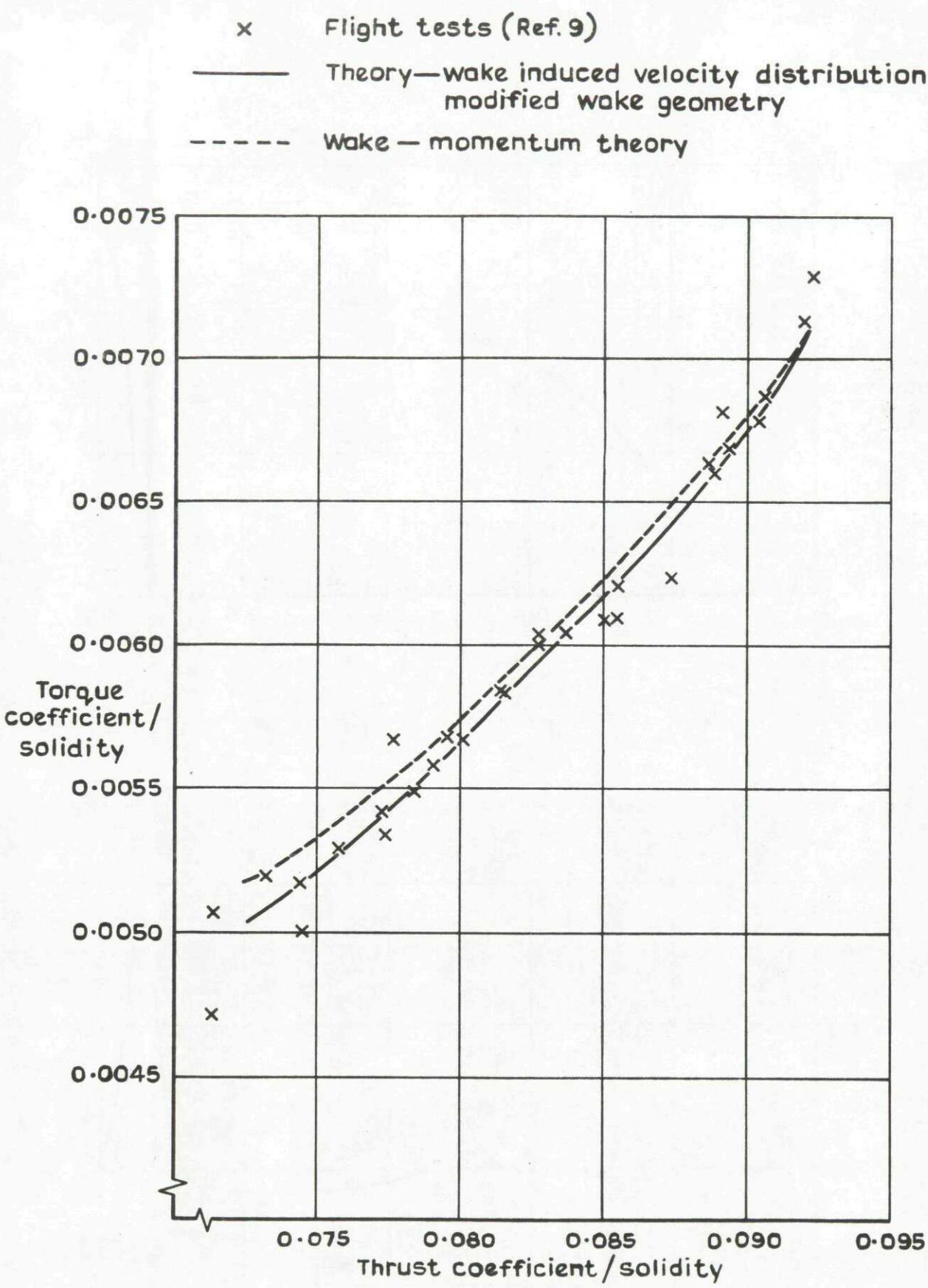

Fig.18 Calculated Wessex hover performance using the wake induced velocities with the tip vortex displacement increased

Printed in England for Her Majesty's Stationery Office by the Royal Aircraft Establishment, Farnborough. Dd. 289030 K4 2/76.

ARC CP No.1341
June 1974

Young, C.

533.662.6 :
533.6.013.67 :
533.6.048.3 :
533.6.013.16 :
533.6.048.1

THE PREDICTION OF HELICOPTER ROTOR HOVER PERFORMANCE USING A PRESCRIBED WAKE ANALYSIS

A method of calculating the performance of a helicopter rotor in the hover is presented. The method combines the downwash velocity distribution induced by a contracting spiral vortex wake with strip element-momentum theory. The shape of the wake takes a prescribed geometry developed from an extensive series of model tests made in the USA.

The predicted thrust and power is in good agreement with measurements made on model and full scale rotors provided that the aerofoil data is sufficiently well defined. The calculated load distribution along the blade is also compared with measurements made on Wessex helicopters. The load distribution is shown to be very sensitive to a light wind but theory compares well with experiment when this effect is eliminated.

The hover performance predicted using only the wake induced velocity distribution is also discussed. The rotor performance is shown to be too sensitive to the geometry of the wake for the method to be used as a design tool with confidence, and the mathematical representation of the wake needs improving.

ARC CP No.1341
June 1974

Young, C.

533.662.6 :
533.6.013.67 :
533.6.048.3 :
533.6.013.16 :
533.6.048.1

THE PREDICTION OF HELICOPTER ROTOR HOVER PERFORMANCE USING A PRESCRIBED WAKE ANALYSIS

A method of calculating the performance of a helicopter rotor in the hover is presented. The method combines the downwash velocity distribution induced by a contracting spiral vortex wake with strip element-momentum theory. The shape of the wake takes a prescribed geometry developed from an extensive series of model tests made in the USA.

The predicted thrust and power is in good agreement with measurements made on model and full scale rotors provided that the aerofoil data is sufficiently well defined. The calculated load distribution along the blade is also compared with measurements made on Wessex helicopters. The load distribution is shown to be very sensitive to a light wind but theory compares well with experiment when this effect is eliminated.

The hover performance predicted using only the wake induced velocity distribution is also discussed. The rotor performance is shown to be too sensitive to the geometry of the wake for the method to be used as a design tool with confidence, and the mathematical representation of the wake needs improving.

Cut here

ARC CP No.1341
June 1974

Young, C.

533.662.6 :
533.6.013.67 :
533.6.048.3 :
533.6.013.16 :
533.6.048.1

THE PREDICTION OF HELICOPTER ROTOR HOVER PERFORMANCE USING A PRESCRIBED WAKE ANALYSIS

A method of calculating the performance of a helicopter rotor in the hover is presented. The method combines the downwash velocity distribution induced by a contracting spiral vortex wake with strip element-momentum theory. The shape of the wake takes a prescribed geometry developed from an extensive series of model tests made in the USA.

The predicted thrust and power is in good agreement with measurements made on model and full scale rotors provided that the aerofoil data is sufficiently well defined. The calculated load distribution along the blade is also compared with measurements made on Wessex helicopters. The load distribution is shown to be very sensitive to a light wind but theory compares well with experiment when this effect is eliminated.

The hover performance predicted using only the wake induced velocity distribution is also discussed. The rotor performance is shown to be too sensitive to the geometry of the wake for the method to be used as a design tool with confidence, and the mathematical representation of the wake needs improving.

Cut here

DETACHABLE ABSTRACT CARDS

DETACHABLE ABSTRACT CARDS

1976

Published by
HER MAJESTY'S STATIONERY OFFICE

Government Bookshops
49 High Holborn, London WC1V 6HB
13a Castle Street, Edinburgh EH2 3AR
41 The Hayes, Cardiff CF1 1JW
Brazennose Street, Manchester M60 8AS
Southey House, Wine Street, Bristol BS1 2BQ
258 Broad Street, Birmingham B1 2HE
80 Chichester Street, Belfast BT1 4JY
Government Publications are also available through booksellers

C.P. No. 1341

ISBN 011 470951 3